

1 **Assessing vegetation structure and ANPP dynamics in a**
2 **grassland-shrubland Chihuahuan ecotone using NDVI-**
3 **rainfall relationships**

4
5 **M. Moreno-de las Heras¹, R. Díaz-Sierra², L. Turnbull¹, J. Wainwright¹**
6 [1]{Department of Geography, Durham University, Durham DH1 3LE, United Kingdom}
7 [2]{Mathematical and Fluid Physics Department, Faculty of Sciences, UNED, Madrid 28040,
8 Spain}
9 Correspondence to: M. Moreno-de las Heras (mariano.moreno-de-las-heras@durham.ac.uk)

10

11 **Abstract**

12 Climate change and the widespread alteration of natural habitats are major drivers of
13 vegetation change in drylands. In the Chihuahuan Desert, large areas of grasslands dominated
14 by perennial grass species have transitioned over the last 150 years to shrublands dominated
15 by woody species, accompanied by accelerated water and wind erosion. Multiple mechanisms
16 drive the shrub-encroachment process, including precipitation variations, land-use change,
17 and soil erosion-vegetation feedbacks. In this study, using a simple ecohydrological
18 modelling framework, we show that herbaceous (grasses and forbs) and shrub vegetation in
19 drylands have different responses to antecedent precipitation due to functional differences in
20 plant growth and water-use patterns. Therefore, shrub encroachment may be reflected in the
21 analysis of landscape-scale vegetation-rainfall relationships. We analyze the structure and
22 dynamics of vegetation at an 18 km² grassland-shrubland ecotone in the northern edge of the
23 Chihuahuan Desert (McKenzie Flats, Sevilleta National Wildlife Refuge, NM, USA) by
24 investigating the relationship between decade-scale (2000-13) records of remotely sensed
25 vegetation greenness (MODIS NDVI) and antecedent rainfall. NDVI-rainfall relationships
26 show a high sensitivity to spatial variations on dominant vegetation types across the
27 grassland-shrubland ecotone, and provide ready biophysical criteria to (a) classify landscape
28 types as a function of the spatial distribution of dominant vegetation, and to (b) decompose
29 the NDVI signal into partial components of annual net primary production (ANPP) for

Deleted: A classic case of vegetation change is the shrub-encroachment process that has been taking place over the last 150 years i

Deleted: where

Deleted: (black grama, *Bouteloua eriopoda*, and blue grama, *B. gracilis*)

Deleted: (creosotebush, *Larrea tridentata*, and mesquite, *Prosopis glandulosa*)

Deleted: exogenous triggering factors such as

Deleted: and

Deleted: endogenous amplifying mechanisms brought about by

Deleted: simulations of plant biomass dynamics with a simple

Deleted: indicate

Deleted: , and t

Deleted: medium-resolution remote sensing of

Deleted: precipitation

Deleted: Spatial evaluation of NDVI-rainfall relationship at the studied ecotone indicates that herbaceous vegetation shows quick growth pulses associated with short-term (previous 2 months) precipitation, while shrubs show a slow response to medium-term (previous 5 months) precipitation. We use these relationships to

Deleted: primary production

1 herbaceous vegetation and shrubs. Analysis of remote-sensed ANPP dynamics across the
2 study site indicates that plant growth for herbaceous vegetation is particularly synchronized
3 with monsoonal summer rainfall. For shrubs, ANPP is better explained by winter plus
4 summer precipitation, overlapping the monsoonal period (June to September) of rain
5 concentration. Our results suggest that shrub encroachment has not been particularly active in
6 this Chihuahuan ecotone for 2000-13. However, future changes in the amount and temporal
7 pattern of precipitation (i.e. reductions in monsoonal summer rainfall and/or increases in
8 winter precipitation) may enhance the shrub-encroachment process. particularly in the face of
9 expected upcoming increases in aridity for desert grasslands of the American Southwest.

Deleted: across the study site

10

11 **1 Introduction**

12 Land degradation is pervasive across many dryland regions, which cover over 40% of the
13 Earth's surface and account for about 30% of global terrestrial net primary productivity,
14 globally supporting about 2.5 billion inhabitants (Millennium Ecosystem Assessment, 2005).

15 Over recent decades these dryland regions have experienced growing human and climatic
16 pressures. The most dramatic landscape alterations resulting from these pressures are those
17 associated with desertification, which are perceived as catastrophic and largely irreversible
18 changes that can ultimately lead to relatively barren ecosystem states (Schlesinger et al.,
19 1990; Okin et al., 2009). A common form of vegetation change in drylands involves the
20 encroachment of desert shrub species into arid and semi-arid grasslands, which has already
21 affected more than 250 million hectares worldwide throughout the US, South America,
22 Southern Africa and Australia (D'Odorico et al., 2012; Turnbull et al., 2014).

23 A classic case of vegetation shift is the shrub-encroachment process that has been taking place
24 over the last 150 years in the Chihuahuan Desert in south-western USA and northern Mexico,
25 where large areas of grasslands dominated by C₄ perennial grass species (black grama,
26 *Bouteloua eriopoda*, and blue grama, *B. gracilis*) have been replaced by shrublands
27 dominated by C₃ desert shrub species (mainly creosotebush, *Larrea tridentata*, and honey
28 mesquite, *Prosopis glandulosa*). These changes in vegetation have been accompanied by
29 accelerated water and wind erosion (for example, Schlesinger et al., 1990; Wainwright et al.,
30 2000; Mueller et al., 2007; Turnbull et al., 2010a; Ravi et al., 2010). A complex range of
31 mechanisms have been suggested to explain the occurrence of this vegetation transition,
32 including external drivers that initiate the transition, and endogenous soil erosion-vegetation

Deleted: We further apply remote-sensed annual net primary production (ANPP) estimations and landscape type classification to explore the influence of inter-annual variations in seasonal precipitation on the production of herbaceous and shrub vegetation. Our results suggest that

Deleted: comprising

Deleted:

Deleted: in

Deleted: Causes for concern have increased during the last decades due to

Deleted: in these dryland regions

Deleted: largely irreversible

Deleted: .

Deleted: phenomenon

Deleted: the incidence of

Deleted: factors

Deleted: ecosystem transition

Deleted: amplifying mechanisms of vegetation change brought about by

1 feedbacks that further drive vegetation change (Turnbull et al., 2012). These internal
2 feedbacks strongly alter the organization and distribution of both vegetation and soil resources
3 (i.e. substrate, soil moisture and nutrients), strengthening the vegetation-change process (Okin
4 et al., 2009; Turnbull et al., 2010b, 2012; Stewart et al., 2014).

5 The onset of the grassland-shrubland transition in the Chihuahuan Desert is thought to have
6 started with the introduction of large numbers of domestic grazers, which may have favored
7 the establishment of pioneer shrubs via the creation of gaps (Buffington and Herbel, 1965;
8 van Auken, 2000; Webb et al., 2003) and via a reduction in the frequency and intensity of
9 natural wildfires (D'Odorico et al., 2012). Changing rainfall amount and frequency has also
10 been invoked as one of the major external drivers of shrub encroachment, which may
11 contribute to vegetation change by shifting competitive plant physiological advantages of
12 grass and desert shrub species (Gao and Reynolds, 2003; Snyder and Tartowsky, 2006;
13 Throop et al., 2012). However, there remains a lack of consensus regarding changes in rainfall
14 in the southwest USA over recent decades. Whilst Petrie et al. (2014) found no significant
15 changes in precipitation at the Sevilleta Long Term Ecological Research Site in central New
16 Mexico, other studies have reported significant increases in both annual and winter
17 precipitation at the Jornada Experimental Range in southern New Mexico, but concurrent
18 decreases in the size of discrete precipitation events (Wainwright, 2006; Turnbull et al.,
19 2013).

20 Comprehensive understanding of how desert grasslands are responding to the present
21 variability on both climate and land use is critical for environmental management, especially
22 in consideration of uncertainty regarding future climate change across many dryland regions.
23 Remote sensing of vegetation provides a valuable source of information for landscape
24 monitoring and forecasting of vegetation change in drylands (Okin and Roberts, 2004;
25 Pennington and Collins, 2007; Moreno-de las Heras et al., 2012). Satellite-derived
26 chlorophyll-sensitive vegetation indices, such as the Normalized Difference Vegetation Index
27 (NDVI), provide important information on vegetation structure (e.g. surface cover,
28 aboveground green biomass, vegetation type) and dynamics over broad spatial domains
29 (Anderson et al., 1993; Peters et al., 1997; Weiss et al., 2004; Pettorelli et al., 2005; Choler et
30 al., 2010; Forzieri et al., 2011).

31 In drylands, where vegetation dynamics are particularly well coupled with rainfall patterns,
32 the relationship between time series of NDVI and precipitation provides specific information

Deleted: Long-term records suggest that the current grassland-shrubland transition in the Chihuahuan Desert

Deleted: facilitated the propagation of desert shrub species by creating gaps of bare soil that

Deleted: . Grazing is also likely to have contributed to reduced shrub mortality by altering

Deleted: precipitation

Deleted: distribution

Deleted: precipitation

Deleted: in

Deleted: Once the shrub-encroachment phenomenon is initiated, the process is further amplified by internal soil erosion-vegetation feedbacks. These internal feedbacks strongly alter the organization and distribution of both vegetation and soil resources (i.e. substrate, soil moisture and nutrients), strengthening the vegetation-change process (Okin et al., 2009; Turnbull et al., 2010a, 2012; Stewart et al., 2014).

Deleted: very

Deleted: Multi-temporal series of coarse- and medium-resolution NDVI, now routinely and freely available from several satellite-borne sensors (e.g. the Advanced Very High Resolution Radiometer, NOAA-AVHRR, the Moderate Resolution Imaging Spectro-radiometer, MODIS), offer powerful tools for the analysis of the impacts of environmental change on the distribution and dynamics of arid and semiarid vegetation (Huete et al., 2002; Holm et al., 2003; Weiss et al., 2004; Pennington and Collins, 2007; Forzieri et al., 2011).

1 on the use of water for the production and maintenance of plant biomass (Pennington and
2 Collins, 2007; Notaro et al., 2010; Veron and Paruelo, 2010). Investigations of the
3 relationships between NDVI and rainfall suggest that arid and semi-arid vegetation responds
4 to antecedent (or preceding cumulative) precipitation rather than to immediate rainfall, since
5 plant growth is affected by the history of available soil moisture (Al-Bakri and Suleiman,
6 2004; Schwinnig and Sala, 2004; Evans and Geerken, 2004; Moreno-de las Heras et al.,
7 2012). The length (or number of days) of antecedent rainfall that best explains the NDVI (or
8 green biomass) dynamics of dryland vegetation (hereafter optimal length of rainfall
9 accumulation, Olr) appears to be site-specific and strongly dependent on vegetation type
10 (Evans and Geerken, 2004; Prasad et al., 2007; Garcia et al., 2010). Herbaceous vegetation
11 (i.e. grass and forb life-forms) and shrubs usually show important differences in the patterns
12 of vegetation growth and water-use, which mediate the responses of plant biomass to rainfall
13 in drylands (Ogle and Reynolds, 2004; Gilad et al., 2007; Pennington and Collins, 2007;
14 Forzieri et al., 2011; Stewart et al., 2014). Thus, the study of the relationship between the
15 NDVI and rainfall may offer important clues for detecting broad-scale landscape changes
16 involving grassland-shrubland transitions in arid and semi-arid landscapes.

17 The aim of this study is to analyze vegetation structure and dynamics at a Chihuahuan
18 grassland-shrubland ecotone (McKenzie Flats, Sevilleta National Wildlife Refuge, New
19 Mexico, USA). To fulfil this aim we explore the relationship between decade-scale (2000-13)
20 records of remote-sensed vegetation greenness (MODIS NDVI) and rainfall. Our analysis is
21 based on a new approach that examines characteristic NDVI-rainfall relationships for
22 dominant vegetation types (i.e. herbaceous vegetation and woody shrubs) to investigate the
23 organization and dynamics of vegetation as a way of evaluating how the shrub-encroachment
24 process occurs.

25 This paper is organized in two parts. First, we present the conceptual underpinning and
26 theoretical basis of our study, by using a simple, process-based ecohydrological model to
27 illustrate the biophysical control of the relationship between plant biomass dynamics and
28 antecedent rainfall for dryland herbaceous and shrub vegetation. Secondly, we empirically
29 determine reference optimal lengths of rainfall accumulation (in days) for herbaceous and
30 shrub vegetation (Olr_{hv} and Olr_s) in a 18 km² Chihuahuan ecotone, and use these vegetation-
31 type specific NDVI-rainfall metrics to (i) analyze the spatial organization and dynamics of net
32 primary production (NPP) for herbaceous vegetation and shrubs, and to (ii) explore the impact

Deleted: NDVI-rainfall signature of vegetation

Deleted: precipitation

Deleted: , resulting from environmental change

Deleted: landscape

Deleted: by studying

Deleted: precipitation

Deleted: use

Deleted: the conceptual underpinning and theoretical basis of our study:

Deleted: precipitation

Deleted: fine

Deleted: NDVI-rainfall signatures

Deleted: of

Deleted: for

Deleted: broad

Deleted: further

Deleted: relationships between vegetation greenness and antecedent precipitation

Deleted: :

Deleted: to

Deleted: to

1 of inter-annual variations in seasonal rainfall on the dynamics of vegetation production at the
2 grassland-shrubland ecotone.

Deleted: precipitation

3

4 **2 Theoretical basis: herbaceous and shrub plant biomass-rainfall**
5 **relationships in drylands**

6 Dryland herbaceous vegetation (i.e. grass and forb life-forms) and shrubs usually exhibit
7 important differences in the patterns of vegetation growth and water-use. Herbaceous
8 vegetation typically shows quick and intense growth pulses synchronized with major rainfall
9 events, while the dynamics of plant biomass for shrubs is generally less variable in time
10 (Sparrow et al., 1997; Lu et al., 2003; Garcia et al., 2010). These dissimilar growth responses
11 are controlled biophysically by the different plant growth and mortality rates associated with
12 herbaceous vegetation and shrubs. While grasses and forbs are associated with high rates of
13 plant growth and mortality, shrubs are associated with comparatively lower plant growth and
14 mortality rates (Ogle and Reynolds, 2004; Gilad et al., 2007).

Deleted: precipitation

15 We use a simplified version of the dynamic ecohydrological model developed by Rietkerk et
16 al. (2002) to illustrate conceptually how the vegetation-specific rates of plant growth and
17 mortality control the relationship between the dynamics of aboveground biomass and
18 antecedent rainfall for herbaceous vegetation and shrubs in drylands. The model consists of
19 two interrelated differential equations; one describing the dynamics of vegetation
20 (aboveground green biomass, B , g m⁻²) and the other describing soil-moisture dynamics (soil-
21 water availability, W , mm).

Deleted: precipitation

Deleted: plant

22 Changes in plant biomass are controlled by plant growth and mortality:

23
$$\frac{dB}{dt} = g_{max} \frac{W-W_0}{W+k_w} B - mB, \quad (1)$$

24 where plant growth is a saturation function of soil-moisture availability, and is determined by
25 the maximum specific plant-growth rate (g_{max} , day⁻¹), the permanent wilting point or
26 minimum availability of soil moisture for vegetation growth (W_0 , mm), and a half saturation
27 constant (k_w , mm). Plant senescence (biomass loss) is controlled by a plant-specific mortality
28 coefficient (m , day⁻¹).

29 Soil-water dynamics are controlled by rainfall infiltration, plant transpiration, and soil-
30 moisture loss due to both deep drainage and direct evaporation:

1
$$\frac{dW}{dt} = P \frac{B+k_i \cdot i_0}{B+k_i} - c g_{max} \frac{W-W_0}{W+k_w} B - r_w W, \quad (2)$$

2 where water infiltration is modelled as a saturation function of plant biomass, characterized
 3 by the minimum proportion of rainfall infiltration in the absence of vegetation (i_0 ,
 4 dimensionless), a half saturation constant (k_i , g m⁻²) and daily precipitation (P , mm day⁻¹).
 5 Plant transpiration is controlled by plant growth, and is modulated by a plant-water-
 6 consumption coefficient (c , 1 g⁻¹). Finally, water losses to both deep drainage and direct
 7 evaporation are modeled as a linear function of soil-water availability, with a rate r_w (day⁻¹).
 8 A Maple 9.5 (Maplesoft, Waterloo, Canada) code for this model is available for download as
 9 online supporting material of this article ([Code 1](#)).

10 Two sets of plant-growth and mortality coefficients were applied to this model to simulate
 11 vegetation dynamics for a herbaceous species ($g_{max}=0.32$ day⁻¹, $m=0.05$ day⁻¹) and a shrub
 12 ($g_{max}=0.12$ day⁻¹, $m=0.03$ day⁻¹), following criteria established in previous studies (Ogle and
 13 Reynolds, 2004; Gilad et al., 2007). Plant-biomass dynamics for these two vegetation types
 14 (Fig. 1a) were modelled using a north Chihuahuan Desert 15-year daily precipitation series
 15 obtained at the Sevilleta National Wildlife Refuge (Sevilleta LTER,
 16 <http://sev.lternet.edu/data/sev-1>; mean annual rainfall 238 mm) and a set of parameters
 17 obtained from literature suited to dryland environments: $W_0=0.05$ mm, $k_w=0.45$ mm,
 18 $k_i=180$ g m⁻², $i_0=0.20$, $c=0.11$ g⁻¹, $r_w=0.1$ day⁻¹ (Rietkerk et al., 2002; Gilad et al., 2007;
 19 Saco and Moreno-de las Heras, 2013).

20 Using this model, we explored the strength of the plant biomass-precipitation relationship as a
 21 function of the length of rainfall accumulation (Fig 1b). We have applied Pearson's R
 22 correlation between the simulated plant biomass for both the herbaceous and the shrub species
 23 and antecedent rainfall series using various lengths of rainfall accumulation; i.e. for any time
 24 t_i in the plant biomass series, the rainfall in the preceding day (t_{i-1}), the cumulative rainfall in
 25 the two preceding days ($t_{i-1:i-2}$), in the three preceding days ($t_{i-1:i-3}$) and so on. Modelling
 26 results show that the plant biomass-rainfall correlation is maximized at 52 days of cumulative
 27 rainfall for the simulated herbaceous species ($Olr_{hv}=52$ days) and is maximized at 104 days
 28 of cumulative rainfall for the modeled shrub species ($Olr_s=104$ days; Fig. 1b). This result
 29 indicates that the simulated herbaceous species responds to short-term (~ two months)
 30 antecedent rainfall for the production of plant biomass whilst the simulated shrub species
 31 responds to a longer period of antecedent precipitation to support plant dynamics. [Here](#).

Deleted: contrasted
Deleted: e aforementioned
Deleted: n

Deleted: plausible

Deleted: precipitation
Deleted: precipitation
Deleted: precipitation

Deleted: T

Formatted: Font: Italic
Formatted: Font: Italic, Subscript
Deleted: and
Deleted: herbaceous and
Deleted: , respectively
Formatted: Font: Italic
Formatted: Font: Italic, Subscript

1 *ARain_{hv}* and *ARain_s* are defined as the antecedent rainfall series that optimize those
2 vegetation-type specific relationships (i.e. time series of precedent rainfall with accumulation
3 lengths *Olr_{hv}* for herbaceous vegetation and *Olr_s* for shrubs, Fig. 1a). Further analysis using a
4 range of plausible values for the plant-mortality and maximum plant-growth coefficients (Fig.
5 1c) indicates that *Olr* increases largely by reducing the characteristic plant-mortality and
6 growth rates of vegetation, and therefore suggests a strong influence on vegetation type.
7 Sensitivity analysis of *Olr* to other model parameters (Supplementary Fig.1 in the online
8 supporting information of this study) indicates that *W₀*, *k_w*, *k_f*, and *c* have negligible effects on
9 simulated *Olr* values. Reductions on bare soil infiltration (*i₀*) and increases on water loss by
10 direct evaporation and/or deep drainage (*r_w*) can impact *Olr_{hv}* and *Olr_s* values, ultimately
11 amplifying the differences we obtained between vegetation types. Other factors not explicitly
12 considered in our model, such as differences in root structure, may also reinforce herbaceous
13 and shrub differences in time-scale plant responses to antecedent precipitation (Reynolds et
14 al., 2004; Collins et al., 2014).

Deleted: the rainfall accumulation length (in days) of the antecedent precipitation series which maximizes the plant biomass-rainfall signature of vegetation, $R_{AL_{max}}$ strongly

Deleted: high sensitivity

Deleted: to

15 The simple model presented in this study provides a good starting point for addressing general
16 differences in plant responses to antecedent precipitation for different vegetation types in
17 drylands. Overall, our modelling results illustrate conceptually the distinct dependence of the
18 relationship between plant biomass and antecedent precipitation on vegetation type,
19 particularly when comparing the dynamics of dryland herbaceous and shrub vegetation.

Deleted: These

20 In the following part of this study, we empirically determine and use metrics of reference
21 vegetation-type specific relationships between aboveground green biomass and antecedent
22 rainfall (i.e. optimal *Olr_{hv}* and *Olr_s* lengths, and corresponding *ARain_{hv}* and *ARain_s* series) to
23 explore the spatial organization and NPP dynamics of herbaceous and shrub vegetation at a
24 semi-arid grassland-shrubland ecotone.

Deleted: precipitation

26 3 Materials and methods

27 3.1 Study area

28 This study is conducted in the Sevilleta National Wildlife Refuge (SNWR), central New
29 Mexico, USA, the location of the Sevilleta Long Term Ecological Research (LTER) site. The
30 SNWR is located in the northern edge of the Chihuahuan Desert, and is a transition zone
31 between four major biomes: the Chihuahuan Desert, the Great Plains grasslands, the Colorado

1 Plateau steppe, and the Mogollon coniferous woodland (Fig. 2a). Livestock grazing has been
2 excluded from the SNWR since 1973, following 40 years of rangeland use. Due to the biome-
3 transition nature of the SNWR, minor variations in environmental conditions and/or human
4 use can result in large changes in vegetation composition and distribution at the refuge
5 (Turnbull et al., 2010b). Analysis of aerial photographs and soil-carbon isotopes indicate that
6 the extent of desert shrublands has considerably increased over the grasslands in regions of
7 the SNWR over the last 80 years (Gosz, 1992; Turnbull et al., 2008).

Deleted: Hochstrasser et al., 2002;

Deleted: 2010a

Deleted: Of particular interest is the shrub-encroachment process that has affected the SNWR over the last century.

8 Our study area is an 18 km² grassland-shrubland ecotone within the McKenzie Flats, an area
9 of gently sloping terrain on the eastern side of the SNWR (Fig. 2b). This study area extends
10 over two LTER Core Sites established in 1999 (Fig. 2c): a desert shrubland (Creosotebush
11 SEV LTER Core Site) dominated by creosotebush, and a grassland (Black Grama SEV LTER
12 Core Site) dominated by black grama. The central and northeastern parts of the study area are
13 mixed black and blue grama (*Bouteloua eriopoda* and *B. gracilis*, respectively) grasslands.

Deleted: despite the exclusion of cattle in the area since 1973, which suggests that other factors and mechanisms (e.g. rainfall variations, erosion-vegetation feedbacks) may have contributed to the observed vegetation change

Deleted: c

Deleted: s

Deleted: Broadly, t

14 The abundance of creosotebush (*Larrea tridentata*) in the grasslands is generally low,
15 although smaller shrubs and succulents (e.g. *Gutierrezia sarothrae*, *Ephedra torreyana*, *Yucca*
16 *glauca*, *Opuntia phaeacantha*) can be common. The abundance of perennial grass species
17 decreases to the southern and southwestern parts of the study area, where creosotebush stands
18 are widely distributed with in general low (although variable in time) amounts of annual forbs
19 and grasses. Soils are Turney sandy loams (Soil Survey Staff, 2010) with about 60% sand and
20 20% silt content (Muldavin et al., 2008; Turnbull et al., 2010b). The climate is semi-arid, with
21 mean annual precipitation of ~240 mm that is made up of 57% falling in the form of high-
22 intensity convective thunderstorms during the summer monsoon (June to September) and the
23 remainder being received as low-intensity frontal rainfall and snow (October to May). Mean
24 annual daily temperature is 14°C, with a winter average of 6°C and a summer average of
25 24°C. Daily air temperature rises over 10°C in the beginning of April, leading to the onset of
26 the yearly cycles of vegetation growth (Weiss et al., 2004). Vegetation growth in the study
27 area generally peaks between July and September, coinciding with the summer monsoon
28 (Muldavin et al., 2008).

Deleted: Conversely, t

Deleted: importantly

Deleted: clumps

Deleted: 2010a

Deleted: . 1997-2013 local meteorological records indicate that mean annual precipitation is about

Deleted: .

Deleted: with

Deleted: 43% coming in the form of

29 **3.2 Vegetation measurements (remote sensed and ground based) and rainfall 30 data**

31 We use temporal series of NDVI as a proxy of aboveground green biomass in our study area.
32 NDVI is a remote-sensed chlorophyll-sensitive vegetation index that correlates with green

Deleted: broad-scale

Deleted: dynamics

1 biomass in semi-arid environments (Anderson et al., 1993; Huete et al., 2002; Veron and
2 Paruelo, 2010). Differences in soil background brightness can generate important
3 uncertainties in relating NDVI levels to dryland vegetation, especially when vegetation cover
4 is low and soil type is heterogeneous in space (Okin et al., 2001). Despite these uncertainties,
5 multiple studies have demonstrated the usefulness of NDVI for examining primary production
6 and vegetation structure in arid and semi-arid ecosystems (for example, Weiss et al., 2004;
7 Choler et al., 2010; Moreno-de las Heras et al., 2012), and particularly in Chihuahuan
8 landscapes with sparse vegetation (30-50% cover) similar to those included in this study
9 (Peters and Eve, 1995; Peters et al., 1997; Pennington and Collins, 2007; Notaro et al., 2010).
10 We compiled decade-scale (2000-13) series of NDVI with a 16-day compositing period from
11 the MODIS Terra satellite (MOD13Q1 product, collection 5, approx. 250 m resolution). We
12 used the NASA Reverb search tool (NASA EOSDIS, <http://reverb.echo.nasa.gov/>) to
13 download the corresponding MODIS tiles. The data were re-projected to UTM WGS84 and
14 further resampled to fit our 18-km² study area (335 pixels; 231.5 m pixel resolution after re-
15 projection to UTM coordinates). We checked the reliability layer of the acquired MODIS
16 products and discarded those NDVI values that did not have the highest quality flag value
17 (less than 1 % of data). Missing values were interpolated using a second order polynomial. To
18 reduce inherent noise, the NDVI time series were then filtered by applying a Savitzky-Golay
19 smoothing algorithm, as recommended by Choler et al. (2010).

Deleted: However

20 To validate remote sensing analysis of the spatial distribution of vegetation types, the
21 dominance of herbaceous vegetation, shrubs, perennial grass, forbs, and creosotebush plants
22 was recorded at a set of 27 control points (Fig. 2c) using the point-intercept method (Godin-
23 Alvarez et al., 2009). Vegetation presence/absence of the aforementioned vegetation types
24 was recorded every metre using a 2-cm diameter, 1.2-m tall, metal rod pointer along five 50-
25 m long linear transects that were laid at each control point at random directions (without
26 overlapping). Dominance was determined as the relative abundance of a particular vegetation
27 type in relation to the total amount of vegetated points found per linear transect.

Deleted: To reduce inherent noise in the
NDVI time series, w

Deleted: T

28 Reference information on aboveground net primary production (NPP) was obtained from a
29 pre-existing decade-scale (2000-11) dataset (Sevilleta LTER, <http://sev.lternet.edu/data/sev-182>). This dataset was recorded in a set of 10 sampling webs distributed within the Black
30 Grama and Creosotebush SEV LTER Core Sites (five webs per Core Site, Fig. 2c). Each
31 sampling web consisted of four 25-m² square sub-plots located in each cardinal direction

Deleted: the

Deleted: analysis

Deleted: ground information on

Deleted: spatial distribution of vegetation
types

Deleted: distributed within the study area

Deleted: . The dominance of herbaceous
vegetation, shrubs, perennial grass, forbs,
and creosotebush plants was determined in
each control point by applying

Deleted: , whereby five 50-m long linear
transects were laid at each control point at
random directions (without overlapping). P

Deleted: c

Deleted: s

1 around the perimeter of a 200-m diameter circle, with four 1-m² quadrats spatially distributed
2 in the internal corners of the 25-m² sub-plots. A detailed description of the methods that were
3 applied for the development of the SEV LTER field NPP dataset can be found in Muldavin et
4 al. (2008). Briefly, species-specific plant standing biomass was estimated three times per year
5 (in February-March, May-June and September-October) using allometric equations, and NPP
6 was calculated seasonally for spring (the difference in plant biomass from March to May),
7 summer (from June to September), and fall/winter (from October to February). For this study,
8 we have used lumped records of annual net primary production (ANPP) for herbaceous
9 vegetation and shrubs that were spatially averaged at the **Core Site** scale. ANPP for each
10 yearly cycle of vegetation growth has been calculated as the sum of the seasonal NPP records
11 (i.e. spring + summer + fall/winter).

12 Daily rainfall information for this study was obtained from an automated meteorological
13 station located in the study site (the Five Points weather station, SEV LTER, Fig. 2c; Sevilleta
14 LTER, <http://sev.lternet.edu/data/sev-1>). The meteorological station is equipped with a rain
15 gauge that records precipitation on a 1-minute basis during periods of rain.

16 **3.3 Reference NDVI-rainfall metrics for herbaceous vegetation and shrubs**

17 We explored reference NDVI-rainfall relationships for herbaceous vegetation and shrubs in
18 the Black Grama and Creosotebush SEV LTER Core Sites (where vegetation is dominantly
19 herbaceous and shrub, respectively) using the 2000-13 NDVI time series (averaged from five
20 MODIS pixels in each site, covering a total of 1200 m² per site). Pearson's correlations
21 between NDVI and antecedent precipitation series were calculated for the two sites using
22 various lengths of rainfall accumulation (1-300 days). Optimal length of rainfall accumulation
23 for herbaceous vegetation and shrubs (Olr_{hv} and Olr_s , respectively) were then determined as
24 the length of rainfall accumulation (in days) of the antecedent precipitation series that
25 maximized the correlations between NDVI and rainfall in the black grama- and the
26 creosotebush-dominated **Core Sites**, respectively. Growth of non-dominant herbaceous
27 vegetation in arid shrublands can make the detection of shrub-specific NDVI-rainfall metrics
28 (i.e. Olr_s) difficult due to the emergence of secondary Olr_{hv} values, particularly in wet years
29 with strong herbaceous production (Moreno-de las Heras et al., 2012). We applied detailed
30 analysis of the NDVI-rainfall relationships in the Core Sites for each annual cycle of
31 vegetation growth to facilitate discrimination of the Olr_{hv} and Olr_s metrics. Our approach
32 assumes linearity between rainfall and both NDVI values and green biomass, which has been

Deleted: c

Deleted: s

Deleted: signatures of

Deleted: Reference

Deleted: signatures

Deleted: were explored

Deleted: .

Deleted: T

Deleted: time series of

Deleted: were extracted for the two core sites

Deleted: The NDVI-rainfall signatures

Deleted: This approach assumes linearity between rainfall and both NDVI values and green biomass, as it has been broadly demonstrated to occur for dryland vegetation (Evans and Geerten, 2004; Muldavin et al., 2008; Choler et al., 2010; Notaro et al., 2010; Veron and Paruelo, 2010; Moreno-de las Heras et al., 2012). Exploratory data analysis using local records of rainfall, NDVI and field NPP confirmed linearity as a reasonable assumption for the study area.¶

Deleted: types

Deleted: mask

Deleted: the NDVI-rainfall signature of dominant vegetation in mixed landscapes

1 broadly demonstrated to occur for dryland vegetation (Evans and Geerken, 2004; Choler et
2 al., 2010; Notaro et al., 2010; Veron and Paruelo, 2010; Moreno-de las Heras et al., 2012) and
3 particularly in our grassland-shrubland desert ecotone (Pennington and Collins, 2007;
4 Muldavin et al., 2008).

5 The optimal antecedent rainfall series determined in the Core Sites for herbaceous vegetation
6 ($ARain_{hv}$, with Olr_{hv} length of rainfall accumulation) and shrubs ($ARain_s$, with Olr_s rainfall
7 accumulation length) were further used in our 18-km² ecotone to classify landscape types and
8 to decompose local NDVI signals into greenness components for herbaceous and shrub
9 vegetation.

10 3.4 Spatial distribution of vegetation types and landscape classification

11 We applied analysis of the relationship between local series of NDVI and the reference
12 $ARain_{hv}$ and $ARain_s$ antecedent rainfall series to determine the spatial distribution of dominant
13 vegetation and classify landscape types over our 18-km² ecotone study area. This analysis
14 builds on the assumption that spatial variations in the NDVI-rainfall relationship reflect
15 spatial differences in the dominance of vegetation types. We assume that areas dominated by
16 herbaceous vegetation (or shrubs) will show a strong NDVI-rainfall relationship for the
17 herbaceous-characteristic $ARain_{hv}$ (or the shrub-characteristic $ARain_s$) antecedent rainfall
18 series along the study period.

19 The strength of the relationship between NDVI and rainfall (quantified using Pearson's R
20 correlation between NDVI and antecedent precipitation) was calculated for every MODIS
21 pixel in the study area using the reference $ARain_{hv}$ and $ARain_s$ antecedent rainfall series.

22 Correlation values were determined for each cycle of vegetation growth (April-March) in
23 2000-13. In order to reduce data dimensionality, we applied Principal Component Analysis
24 (PCA) using the calculated correlation coefficients as variables for analysis (28 variables
25 resulting from the two vegetation-specific antecedent rainfall series and the 14 growing
26 cycles). We studied further the relationship between the main PCA factors and ground-based
27 dominance of vegetation types using the reference vegetation distribution dataset (27 control
28 points). Finally, we used the empirical relationships between vegetation dominance and the
29 main PCA factors to discriminate differentiated landscape types across the study area: grass-
30 dominated (GD), grass-transition (GT), shrub-transition (ST) and shrub-dominated (SD)
31 landscapes.

Deleted: ¶
Preliminary analysis in this study revealed important mixing effects for the creosotebush-dominated core site, where quick and strong pulses of non-dominant herbs and grasses during wet years masked the shrub-specific NDVI-rainfall signature over the period of analysis. In order to avoid confounding effects (i.e. the mixing of the dominant-shrub and non-dominant herbaceous responses to precipitation) on the identification of the local NDVI-rainfall signatures, correlations between NDVI and antecedent precipitation series (of different rainfall accumulation lengths) were determined independently for each annual cycle of vegetation growth (April-March). We identified the reference signatures for herbaceous and shrub vegetation by determining the series of antecedent precipitation that consistently best explained the NDVI dynamics for the Black Grama and Creosotebush Core Sites across the 2000-13 yearly growing cycles. The reference vegetation-type characteristic antecedent rainfall series ($ARain_{hv}$ and $ARain_s$ for herbaceous vegetation and shrubs, respectively) that were determined in the core sites

Deleted:

Deleted: high strength on the

Deleted: Conversely, a low strength on the NDVI-rainfall relationship consistently obtained across the 2000-13 cycles of vegetation growth for a specific vegetation-characteristic antecedent rainfall series will locally evidence a low activity of the analyzed vegetation type for the study period.

Deleted: independently

Deleted: summarize data variability

Deleted: from this complicated dataset (9380 correlations spatially and temporally distributed in 335 MODIS pixels and 14 growing cycles, respectively)

Deleted: further

Deleted: classify the study area into four homogeneous and

1 **3.5 NDVI decomposition and transformation into herbaceous and shrub ANPP**
 2 **components**

3 Time series of NDVI at any specific location reflects additive contributions of background
 4 soil and the herbaceous and woody shrub components of vegetation (C_{bs} , C_{hv} , and C_s ,
 5 respectively) for that particular site (Lu et al., 2003):

$$6 NDVI(t) = C_{bs}(t) + C_{hv}(t) + C_s(t), \quad (3)$$

Deleted: the
Deleted: the bare
Deleted: background
Deleted: ,
Deleted: vegetation

7 Montandon and Small (2008) carried out *in situ* measurements of field spectra convolved by
 8 the MODIS bands to determine the background soil contribution to NDVI in the SNWR.
 9 They obtained a soil NDVI value of 0.12 for Turney sandy loam soils, which are broadly
 10 distributed across the McKenzie Flats. Analysis of the local MODIS NDVI time series
 11 revealed that this soil-background reference value broadly matches the minimum NDVI
 12 values for our study area. Application of reference soil values in NDVI decomposition and
 13 normalization methodologies provides an efficient standardization approach for characterizing
 14 the background soil baseline, particularly in areas with homogeneous soils (Carlson and
 15 Ripley, 1997; Roderick et al., 1999; Lu et al., 2003; Choler et al. 2010). Soil background

Deleted: of the bare soil component
Deleted: bare
Deleted: Preliminary a
Deleted: soil

16 NDVI may change with soil-moisture content (Okin et al., 2001). Although this effect can be
 17 especially important for dark organic-rich soils, soil-moisture variations have shown a little
 18 impact in desert-type bright sandy and sandy-loam soils, as those represented in the study area
 19 (Huete et al., 1985). Therefore, a constant value of 0.12 was applied to subtract the
 20 background soil baseline (C_{bs}) from the NDVI time series, obtaining a new set of soil-free
 21 series ($NDVI_O$):

Deleted: bare soil component
Deleted: free of the soil background contribution

$$22 NDVI_O(t) = C_{hv}(t) + C_s(t), \quad (4)$$

Deleted: further

23 We applied the reference herbaceous- and shrub-characteristic antecedent rainfall series,
 24 $ARain_{hv}$ and $ARain_s$, to partition single time series of soil-free NDVI ($NDVI_O$) into separate
 25 contributions for herbaceous vegetation (C_{hv}) and woody shrubs (C_s) across our study area.
 26 This approach is based on the assumption that the primary determinant of the dynamics of
 27 both NDVI and green biomass in Chihuahuan landscapes is the rainfall pattern (Huenneke et
 28 al., 2002; Weiss et al., 2004; Muldavin et al., 2008; Pennington and Collins, 2007; Notaro et
 29 al., 2010; Forzieri et al., 2011), and therefore the partial contributions of herbaceous
 30 vegetation and shrubs to NDVI can be estimated as a function of their characteristic
 31 dependency on antecedent rainfall. In other words, we assume that C_{hv} and C_s for any t_i are

Deleted: vegetation-type
Deleted: use of

1 proportional to $ARain_{hv}$ and $ARain_s$. The NDVI components for herbaceous vegetation and
2 shrubs were partitioned using the following two-step NDVI-decomposition procedure ([Maple](#)
3 [9.5 code for analysis provided as online supporting material of this article; Code 2](#)).

4 First, we applied first-order least-squares optimization of the relationship between soil-free
5 NDVI ($NDVI_O$) and the vegetation-type specific antecedent rainfall series ($ARain_{hv}$ and
6 $ARain_s$ for herbaceous vegetation and shrub, respectively):

7 $NDVI_O(t) = h ARain_{hv}(t) + s ARain_s(t)$ (5)

8 where, h and s represent vegetation-type specific rainfall-NDVI conversion coefficients for
9 the herbaceous and shrub components.

10 Secondly, we used the determined coefficients h and s to calculate the weights of C_{hv} and C_s
11 on the time series (i.e. the predicted percentage contribution of each vegetation type over the
12 predicted totals for any t_i). Seasonal variations in other environmental factors (e.g.
13 temperature, day length) may influence NDVI dynamics for Chihuahuan vegetation, shaping
14 the responses of vegetation to precipitation (Weiss et al., 2004; Notaro et al., 2010). In order
15 to preserve the observed seasonality of the original NDVI time series in the decomposed
16 signals for herbaceous and shrub vegetation, the predicted weights (or percentage
17 contributions) of the fitted vegetation components were reassigned to the NDVI levels of the
18 original time series, obtaining the final NDVI components for herbaceous vegetation and
19 shrubs (C_{hv} , and C_s , respectively).

20 The 2000-13 time series of NDVI were decomposed into separate contributions of herbaceous
21 vegetation and shrubs for the Black Grama and Cresotebush SEV LTER Core Sites. We used
22 the reference 2000-11 field NPP dataset to study the relationship between the decomposed
23 NDVI time series and ground-based estimates of herbaceous and shrub NPP for the [Core](#)
24 [Sites](#). The sum of the herbaceous and the shrub NDVI components ($\sum NDVI_{veg.type}$) were
25 calculated for each growing cycle of vegetation (April-March). We further determined the
26 relationships between field ANPP estimates of herbaceous and shrub vegetation and
27 $\sum NDVI_{veg.type}$. Finally, we applied the signal-decomposition procedure to every single NDVI
28 time series of the 335 MODIS pixels contained within our study area. The established [Core](#)
29 [Site](#) NDVI-ANPP relationships were used to estimate herbaceous and shrub ANPP across the
30 18 km² study site.

Deleted: Explorative comparisons revealed that this simple two-step procedure outperformed other more complex NDVI-decomposition methodologies (e.g. artificial neural network, autoregressive and non-linear modeling). In order to facilitate the application of this NDVI-decomposition procedure by other users, the Maple 9.5 (Maplesoft, Waterloo, Canada) code that we developed is available for download as online supporting material of this article.¶

Deleted: overall

Deleted: c

Deleted: s

Deleted: c

Deleted: s

1 **3.6 Spatiotemporal dynamics of vegetation production and impact of**
2 **seasonal precipitation on herbaceous and shrub ANPP**

3 We used the remotely sensed ANPP estimations and landscape-type classification (GD, grass-
4 dominated, GT, grass-transition, ST, shrub-transition, and SD, shrub-dominated landscapes)
5 to analyze the spatiotemporal dynamics of ANPP along our study grassland-shrubland
6 ecotone, applying repeated-measures ANOVA with time as within subjects factor and
7 landscape type as between subjects factor. Departures from sphericity were corrected using
8 the Greenhouse-Geisser F-ratio method for repeated-measures ANOVA (Girden, 1992).
9 2000-13 activity of the shrub-encroachment phenomenon for the established landscape types
10 (GD, GT, ST and SD) was explored applying Pearson's *R* correlation between shrub
11 contribution to total ANPP and time.

12 We used three different seasonal precipitation metrics to analyze the impact of inter-annual
13 variations in seasonal precipitation on the production of herbaceous and shrub vegetation at
14 our ecotone: (i) preceding non-monsoonal rainfall (Rain_{PNM}, from October to May) that takes
15 place before the summer peak of vegetation growth, (ii) summer monsoonal precipitation
16 (Rain_{SM}, from June to September), and (iii) late non-monsoonal rainfall (Rain_{LNM}, from
17 October to March) that takes place at the end of the annual cycles of vegetation growth. The
18 effects of seasonal precipitation on herbaceous and shrub ANPP for the established landscape
19 types (grass-dominated, grass-transition, shrub-transition and shrub-dominated landscapes)
20 were explored by applying Pearson's *R* correlation. Effect significance and size was
21 determined using a general linear model (GLM) that includes the different sources of seasonal
22 precipitation (Rain_{PNM}, Rain_{SM}, and Rain_{LNM}) as covariates, landscape type (LT) as a factor,
23 and the interaction terms between landscape type and seasonal precipitation (LT:Rain_{PNM},
24 LT:Rain_{SM}, and LT:Rain_{LNM}).

25

26 **4 Results**

27 **4.1 Patterns of greenness and reference NDVI-rainfall metrics in the Core**
28 **Sites**

29 Inter- and intra-annual variations of NDVI show similar patterns of vegetation greenness for
30 both the Black Grama and the Creosotebush Core Sites (Fig. 3a). The signal generally peaks
31 slightly in spring (May) and strongly in summer (July-September). The lowest NDVI values

Deleted: I

Deleted: analyze the impact of inter-annual variations in seasonal precipitation on the production of herbaceous and shrub vegetation at our study grassland-shrubland ecotone

Deleted: .

Deleted: T

Deleted: were used in this analysis

Deleted: ¶

Deleted: We explored t

Deleted: further

Deleted: metricssignatures

Deleted: c

Deleted: s

Deleted: Similarly, t

1 are observed between February and April. Summer peaks in NDVI values are, however, less
2 marked in the Creosotebush Core Site. In addition, the NDVI signal for the creosotebush-
3 dominated site generally shows an autumn (October-November) peak that is especially
4 important during particular growing cycles (2000-01, 2001-02, 2004-05, 2007-08, 2009-10).

5 Correlations between NDVI and antecedent precipitation using rainfall accumulation lengths
6 of 1-300 days indicate that an optimal short-term cumulative rainfall period of 57 days best
7 explains the NDVI variations for the dominant herbaceous vegetation of the grassland site
8 (ARain_{hv} antecedent rainfall series, with Olr_{hv} accumulation length; Fig. 3, see also
9 Supplementary Fig. 2 in the online supporting information of this study for details on the
10 annual cycles of vegetation growth). For the Creosotebush Core Site (with dominant shrub
11 vegetation and subordinate forbs and grasses), the short-term, 57-day antecedent rainfall
12 series ARain_{hv} also has an important impact on the strength of the NDVI-rainfall relationship,
13 particularly for three consecutive growing cycles with strong summer precipitation (2006-07,
14 2007-08 and 2008-09, summer precipitation for the period is 40% above the long-term mean).
15 However, the NDVI-rainfall correlation in this shrub-dominated site generally peaks using a
16 much longer optimal cumulative rainfall period of nearly 145 days (ARain_s series, with Olr_s
17 length).

18 4.2 Spatial distribution of vegetation types and landscape classification

19 PCA analysis of the NDVI-rainfall correlation coefficients (per growing cycle) for the
20 reference 57- and 145-day antecedent rainfall series (i.e. ARain_{hv} and ARain_s with Olr_{hv} and
21 Olr_s rainfall accumulation lengths, respectively for all MODIS pixels contained within our
22 study area) shows that PCA factor 1 (about 40% of total data variance) reflects a landscape
23 gradient that discriminates the two reference responses of vegetation greenness to antecedent
24 rainfall (Figs. 4a and 4b). The correlation between the NDVI and the short-term antecedent
25 rainfall series ARain_{hv} increases to the negative side of factor 1 (particularly for growing
26 cycles 2001-02, 2002-03, 2005-06, and 2012-13), while the correlation with the 145-day
27 antecedent rainfall series (ARain_s) increases to the positive side of the this factor (particularly
28 for cycles 2000-01, 2002-03, 2005-06, and 2006-07, Fig. 4b). Analysis of the relationship
29 between PCA factor 1 and vegetation dominance for the ground-based set of control points
30 indicates that this landscape gradient is explained by the field distribution of dominant
31 vegetation types since the dominance of herbaceous vegetation and shrubs increases to the
32 negative and positive side of PCA factor 1, respectively (R² approx. 0.90, Fig. 4c).

Deleted: reached

Deleted: intense

Deleted: various

Deleted:

Deleted: periods

Deleted: nearly

Deleted: for all the annual cycles of vegetation growth

Formatted: Not Superscript/ Subscript

Formatted: Not Superscript/ Subscript

Deleted: b

Deleted: 1

Deleted: d

Deleted:

Deleted: s

Deleted: Figures 4a and 4b display the main

Deleted: results derived from the spatial

Deleted:) in

Deleted:

Deleted: NDVI-rainfall signatures

Deleted: (

Deleted: 57 days)

1 Four different landscape types (GD, GT, ST and SD) are defined in the 18-km² study area as
2 determined by the spatial projection of the relationship between PCA factor 1 and field
3 dominance of herbaceous and shrub vegetation (Figs. 4c and 4d). SD, ST and GT landscapes
4 are distributed in the southwestern part of the study site, while GD landscapes are located in
5 the central and northeastern parts of the area (Figs. 4d and 4e).

6 **4.3 NDVI transformation into herbaceous and shrub ANPP components**

7 Temporal decomposition of NDVI into partial herbaceous and shrub vegetation components
8 results in very different outputs for the reference Black Grama and Creosotebush Core ~~Sites~~
9 (Fig. 5a). The herbaceous component (which is derived from the relationship between NDVI
10 and the reference 57-day antecedent rainfall series, $ARain_{hv}$) prevails in the grass-dominated
11 reference site, ~~whilst~~ the shrub component (which is function of the reference 145-day
12 antecedent rainfall series, $ARain_s$) comprises the leading NDVI fraction in the shrub-
13 dominated reference site.

Deleted: s

Deleted: clearly

Deleted: . Conversely,

14 ~~The annual sums of herbaceous and shrub NDVI components for the reference Core ~~Sites~~~~
15 show a strong linear agreement ($R^2 \geq 0.65$; $P < 0.001$) with ground-based ~~measurements~~ of
16 ANPP (Fig. 5b), while the remote-sensing ANPP estimations yield a root mean square error
17 of 26 g m⁻² (NRMSE 12%, Fig. 5c).

Deleted: In addition, t

Deleted: (per growing cycle)

Deleted: s

Deleted: good and

Deleted: estimations

18 Spatial projection of the reference NDVI-ANPP relationships across the 18 km² study area
19 displays a contrasted distribution of mean 2000-13 ANPP for herbaceous and shrub
20 vegetation (Figs. 5d and 5e). Herbaceous ANPP is mainly distributed in the central and
21 northeastern parts of the study site, ~~contributing to >80% total ANPP~~. Conversely, shrub
22 ANPP is concentrated in the southwestern edge of the study area.

Deleted: c

Deleted: 5d

Deleted: (Fig. 5d)

Deleted: I

23 **4.4 ANPP spatiotemporal dynamics and impact of seasonal precipitation on 24 herbaceous and shrub primary production**

25 ~~Remote-sensed estimations of ANPP are significantly impacted by landscape type~~
26 ($F_{3,334}=48.6$, $P < 0.01$), with grass-dominated sites supporting in general higher levels of
27 vegetation production (Fig. 6a). However, landscape-type effects are variable in time
28 (landscape type x time interaction: $F_{14,1515}=57.2$, $P < 0.01$). Year-to-year variability of ANPP
29 is particularly large for the grass-dominated sites, which show higher levels of ANPP than the
30 transition and shrub-dominated landscapes for highly productive years (Fig. 6a). For growing

1 cycles with low primary production there are no significant ANPP differences or the
2 differences are reversed, with shrub-dominated sites showing higher production than grass-
3 dominated sites (e.g. 2003-04 cycle, Fig. 6a).
4 Analysis of the temporal evolution of shrub contribution to total ANPP along 2000-13 reflects
5 significant (although very weak) positive correlations with time for the grass- and shrub
6 transition landscapes (Fig. 6b). The same analysis at the individual pixel level, however, does
7 not show any significant correlations between shrub contribution to total ANPP and time.

8 Exploratory analysis of the influence of seasonal precipitation on remote-sensed estimations
9 of ANPP indicates different responses for herbaceous and shrub vegetation (Fig. 7).

10 Herbaceous ANPP strongly correlates with monsoonal summer precipitation for all landscape
11 types (Fig. 7a). The slope of the relationship between herbaceous ANPP and monsoonal
12 summer (June-September) precipitation decreases for the shrub-transition and shrub-
13 dominated landscapes. Conversely, shrub ANPP strongly correlates with both preceding non-
14 monsoonal (October-May) and monsoonal summer (June-September) precipitation for all
15 landscape types (Fig. 7b).

16 General linear model results confirm the exploratory observations of the relationships
17 between remote-sensed estimations of ANPP and seasonal precipitation (Table 1). Model
18 results identify both monsoonal summer precipitation ($Rain_{SM}$) and the interaction between
19 $Rain_{SM}$ and landscape type as the most important contributors (effect size, $\eta^2 > 10\%$;
20 $P < 0.001$) to the total variance comprised in ANPP data for herbaceous vegetation. Similarly,
21 non-monsoonal summer precipitation ($Rain_{PNM}$) and monsoonal summer precipitation
22 ($Rain_{SM}$) are identified as the leading contributors to shrub ANPP.

23

24 **5 Discussion**

25 **5.1 Vegetation-growth pattern and reference NDVI-rainfall metrics for** 26 **herbaceous and shrub vegetation**

27 Analysis of time series of NDVI provides important information on the dynamics of
28 vegetation growth in drylands (Peters et al., 1997; Holm et al., 2003; Weiss et al., 2004;
29 Choler et al., 2010). NDVI trends in the grass-dominated site show strong peaks centered in
30 the summer season (Fig. 3a), which agrees with both field and remote-sensed observations of

Deleted: variable

Deleted: 6

Deleted: 6

Deleted: On the other hand

Deleted: 6

Deleted: (LT)

Deleted: signatures

1 the dynamics of aboveground biomass for desert grasslands dominated by *Bouteloua*
2 *eriopoda* and *B. gracilis* in the area (Peters and Eve, 1995; Huenneke et al., 2002; Muldavin
3 et al., 2008; Notaro et al., 2010). For the shrub-dominated site, summer peaks in the NDVI
4 signal are smaller, and for particular years both spring and late-autumn peaks can exceed
5 summer greenness. Accordingly, the timing of plant growth for *Larrea tridentata* (which
6 | dominates the reference shrubland site) has been shown to vary from year to year, since this
7 species has the ability to shift the temporal patterns of vegetation growth to take advantage of
8 changes in resource availability (Fisher et al., 1988; Reynolds et al., 1999; Weiss et al., 2004;
9 Muldavin et al., 2008).

Deleted: largely

10 The analysis of the relationships between NDVI and precipitation provide further insights on
11 plant water-use patterns and, hence, on vegetation function and structure (Pennington and
12 Collins, 2007; Veron and Paruelo, 2010; Notaro et al., 2010; Garcia et al., 2010; Forzieri et
13 al., 2011; Moreno-de las Heras et al., 2012). Temporal trends in NDVI for the reference grass-
14 and shrub-dominated SEV LTER sites are explained by antecedent (or preceding cumulative)
15 rainfall amounts, reflecting the coupling of the history of plant-available soil moisture with
16 vegetation growth (Fig. 3). Correlations between NDVI and precipitation indicate that plant
17 growth pulses for the grass-dominated site are associated with short-term antecedent rainfall
18 ($ARain_{hv}$ series; 57 days optimal length, Olr_{hv}). For the shrub-dominated landscape, vegetation
19 greenness shows a strong association with longer-term antecedent precipitation ($ARain_s$
20 series; 145 days optimal length, Olr_s), although importantly, NDVI dynamics for this site also
21 correlate with the 57-day cumulative rainfall series. Previous work on the analysis of NDVI-
22 rainfall relationships found similar variations in the length of the antecedent rainfall series
23 that best explain the dynamics of vegetation greenness, suggesting that such differences result
24 from site variations in dominant vegetation (Evans and Geerken, 2004; Prasad et al., 2007;
25 Garcia et al., 2010).

Deleted: b

Deleted: (57 days)

Deleted: leaf phenology

Deleted: medium

Deleted: (145 days)

26 Given the strong relationship between time-integrated NDVI values and ground-based ANPP
27 estimations for our site (Fig. 5b), our herbaceous and shrub exploratory modeling results
28 provide a biophysical explanation for the range of variations found in the NDVI-rainfall
29 relationships (Fig. 1). The length of the cumulative precipitation series that optimizes the
30 relationship between plant biomass and antecedent rainfall (Olr) appears to be a function of
31 the characteristic water-use and plant growth pattern of dryland vegetation, that are largely
32 influenced by the plant-growth and mortality rates of vegetation (Fig. 1c). Vegetation growth

Deleted: Our

Deleted: maximizes

Deleted: ultimately

Deleted: controlled

1 and water use strongly differ for herbaceous and shrub life-forms in drylands (Sparrow, 1997;
2 Ogle and Reynolds, 2004; Gilad et al., 2007; Garcia et al., 2010), in which case plant biomass
3 dynamics respond to short-term and long-term antecedent precipitation, respectively (Figs.
4 1a-b). *Olr* variations in the reference SEV LTER Core Sites may, therefore, be expressed as a
5 function of the dominant vegetation types (Fig. 3): the strong and quick responses of
6 greenness to short-term precipitation ($ARain_{hv}$) in the grass-dominated Black Grama Core Site
7 characterize herbaceous growth for the area, while the slow responses of NDVI to medium-
8 term precipitation ($ARain_s$) in the shrub-dominated Cresotebush Core Site define the
9 characteristic pattern of vegetation growth for shrubs in the ecotone. The high correlation
10 between $ARain_{hv}$ and NDVI values in the shrub-dominated Creosotebush Core Site (Fig. 3b)
11 can be explained by the growth of non-dominant herbaceous vegetation (mainly annual
12 forbs), which can be especially important during wet years (Muldavin et al., 2008; Baez et al.,
13 2012). Similarly, Moreno-de las Heras et al. (2012) in dry open-shrublands of central
14 Australia (Olr_s values about 220 days) found the emergence of secondary Olr_{hv} metrics on the
15 study of local NDVI-rainfall relationships (approx. 85 days antecedent rainfall length) caused
16 by the growth of non-dominant herbaceous vegetation. Overall, *Olr* values determined for
17 herbaceous and shrub vegetation in this work are in agreement with the range of characteristic
18 antecedent rainfall series reported in other studies to best describe green biomass dynamics
19 for arid and semi-arid grasslands (1-3 months) and woody shrublands (4-8 months) (Evans
20 and Geerken, 2004; Munkhtsetseg et al., 2007; Garcia et al., 2010; Moreno-de las Heras et al.,
21 2012).

22 5.2 Spatial distribution and net primary production of herbaceous vegetation 23 and shrubs

24 Our results indicate that the relationship between temporal series of remotely sensed NDVI
25 and antecedent precipitation is highly sensitive to spatial differences in dominant vegetation
26 (Fig. 4). The main PCA factor (explaining about 40% variance in data) extracted using the
27 annual NDVI responses (i.e. the Pearson's R coefficients) to the reference 57- and 145-day
28 characteristic antecedent rainfall series ($ARain_{hv}$ and $ARain_s$ series, respectively) accurately
29 discriminates the behavior of herbaceous and shrub vegetation for the 18 km² study area
30 (Figs. 4b-c), hence providing a robust approach for classifying landscapes as a function of the
31 dominance of vegetation types using coarse-grained remotely sensed data (Fig. 4d). This
32 parsimonious approach offers a practical alternative to other more complex remote-sensing

Deleted: v

Deleted: in NDVI-rainfall signatures (i.e. the rainfall accumulation length of the antecedent precipitation series that best explain the NDVI dynamics)

Deleted: c

Deleted: s

Deleted: reference 57-day antecedent rainfall series,

Deleted: the NDVI-rainfall signature of

Deleted: vegetation

Deleted: reference 145-day antecedent rainfall series,

Deleted: signature

Deleted: the short-term (57 days) antecedent rainfall series

Deleted: the length of the reference NDVI-rainfall signatures

Deleted: 2

Deleted: In fact, t

Deleted: variability

1 methodologies for the analysis of the spatial distribution of vegetation types in mixed
2 systems, such as Spectral Mixture Analysis (SMA, Smith et al., 1990), which may be difficult
3 to apply in this Chihuahuan case study since both the mixed nature and fine-grained
4 distribution of vegetation in the area (patches of grass and shrubs are typically $<1\text{ m}^2$ and $0.5\text{--}5\text{ m}^2$, respectively; Turnbull et al. 2010b) can impose serious drawbacks on the detection of
5 reference spectral signatures for pure herbaceous and shrub vegetation using coarse-grained
6 MODIS data. ~~Implementing SMA-based approaches for the analysis of vegetation distribution~~
7 and landscape classification in drylands using medium- and coarse-grained data is very
8 challenging since it requires significant amounts of ancillary data (e.g. lab~~oratory~~-based or
9 field multi-date spectra for vegetation types) to solve data uncertainties generated by surface
10 heterogeneity, which is often not feasible (Somers et al. 2011).

12 The relationships of vegetation greenness to $ARain_{hv}$ and $ARain_s$ also provide criteria for
13 decomposing and transforming the NDVI signal into structural components of primary
14 production for this study. Lu et al. (2003) applied seasonal trend decomposition to partition
15 NDVI into (cyclic) herbaceous and (trend) woody vegetation in Australia. They assumed a
16 long-term weak phenological wave and a strong annual response for determining the shrub
17 and herbaceous components of vegetation, respectively. Our approach relies on the use of
18 differences in biophysical properties of herbaceous and shrub vegetation related to the
19 coupling between vegetation growth and precipitation for decomposing the NDVI signal,
20 rather than apparent differences in the seasonality of vegetation greenness alone. As expected,
21 signal decomposition outcomes indicate that the herbaceous component of the NDVI leads the
22 temporal trends for the grass-dominated reference Black Grama Core Site, while the shrub
23 component largely dominates the NDVI signal for the Creosotebush Core Site (Fig. 5a).

24 ~~Although affected by data dispersion, the annual sums of decomposed NDVI strongly agree~~
25 with field estimations of ANPP for herbaceous and shrub vegetation ($R^2 \geq 0.65$, Fig. 5b),
26 ~~resulting in a small root mean square error for our remote-sensing ANPP estimates (26 g m^{-2} ,~~
27 ~~NRMSE 12%, Fig. 5c)~~ that is within the lower limit of reported errors by other NDVI
28 decomposition studies (for example, Roderick et al., 1999; DeFries et al., 2000; Hansen et al.,
29 2002; Lu et al., 2003; with NRMSE ranging 10–17%). Other dryland studies have found
30 important levels of data dispersion when relating fine-grained field ANPP to coarse-scale
31 NDVI values (Lu et al., 2003; Holm et al., 2003; Pennington and Collins, 2007; Veron and
32 Paruelo, 2010). Major sources of data dispersion for this study are most likely associated with

Deleted: 2010a

Deleted: in fact, i

Deleted: the reference herbaceous- and shrub-characteristic antecedent rainfall series (

Deleted:)

Deleted:

Deleted: In addition, the spatial organization of the remote-sensed estimations of herbaceous and shrub ANPP matches the observed distribution of dominant vegetation types (Figs. 4c-d and 5c-d).

1 the high spatial variability of ANPP in the analyzed systems. For instance, field estimations
2 have shown that ANPP for both grass- and shrub-dominated Chihuahuan landscapes are
3 affected by important levels of spatial variability, primarily due to the patchiness of
4 vegetation cover (Huenneke et al., 2002; Muldavin et al., 2008).

5 **5.3 Spatiotemporal dynamics of ANPP and impact of seasonal precipitation 6 on herbaceous and shrub primary production**

7 Cross-scale interactions between vegetation composition, individual plant characteristics and
8 climatic drivers (e.g. variations in precipitation amount and seasonality) have an important
9 role on determining primary production patterns in arid and semi-arid ecosystems (Peters,
10 2002; Snyder and Tartowsky, 2006; Pennington and Collins, 2007; Notaro et al., 2010; Baez
11 et al., 2013). Analysis of the spatiotemporal dynamics of ANPP in our ecotone indicates that
12 grass-dominated sites, although very importantly affected by year-to-year variability,
13 generally support higher primary production than transition and shrub-dominated landscapes,
14 particularly for wet years with high ANPP levels (Fig. 6a). This result is consistent with other
15 shrub-encroachment studies which have found associations between shrub proliferation and
16 ANPP reductions in dry American grasslands (Huenneke et al., 2002; Knapp et al., 2008).
17 Our results suggest that primary production is differently controlled by seasonal precipitation
18 for herbaceous and shrub vegetation across the 18-km² Chihuahuan Desert ecotone (Fig. 7,
19 Table 1). Monsoonal summer precipitation (June-September) controls ANPP for herbaceous
20 vegetation (Fig. 7a), while ANPP for shrubs is better explained by the preceding year's non-
21 monsoonal (October-May) plus the summer monsoonal precipitation in the present year (Fig
22 7b). Accordingly, field observations of ANPP for Chihuahuan landscapes found that
23 grassland primary production is particularly coupled with monsoonal rainfall, while desert
24 shrublands appear to be less dependent on summer precipitation (Fisher et al., 1988; Reynolds
25 et al., 1999; Huenneke et al., 2002; Muldavin et al., 2008; Throop et al., 2012).

26 Differences in the distribution of rainfall types, soil-moisture dynamics, and rooting habits of
27 dominant plant species may explain the variable impact of seasonal precipitation on
28 herbaceous and shrub ANPP for the studied Chihuahuan landscapes. Monsoonal summer
29 precipitation (July-September, approx. 60% annual precipitation) generally takes place in the
30 form of high-intensity thunderstorms that infiltrate shallow soil depths (top 15-35 cm)
31 (Snyder and Tartowsky, 2006). Summer soil-water resources for plant production are

Deleted: I

Deleted: variations in

Deleted: ,

**Deleted: vegetation composition and
individual plant characteristics**

Deleted:

Deleted: R

**Deleted: of our remote sensing
estimations of ANPP for dominant
vegetation types indicate**

Deleted: 6

Deleted: 6

Deleted: 6

1 ephemeral and strongly affected by evapotranspiration, which typically reduces soil moisture
2 to pre-storm background levels in 4-7 days after rainfall (Turnbull et al., 2010a). C₄ grasses
3 (*Bouteloua eriopoda* and *B. gracilis*), which dominate herbaceous vegetation in the analyzed
4 ecotone, concentrate active roots in the top 30 cm of the soil and intensively exploit
5 ephemeral summer soil moisture for plant growth (Peters, 2002; Muldavin et al., 2008).
6 Preferential spatial redistribution of runoff to grass patches following summer storms further
7 enhances plant production for black and blue grama (Wainwright et al., 2000; Pockman and
8 Small, 2010; Turnbull et al., 2010b).

Deleted: 2010b

9 Non-monsoonal precipitation (about 40% annual precipitation, primarily from November to
10 February) typically falls in the form of long-duration low-intensity frontal rainfall that often
11 percolates to deep soil layers (Snyder and Tartowsky, 2006). *Larrea tridentata*, the dominant
12 C₃ shrub in the studied ecotone, has a bimodal rooting behavior that facilitates the use of both
13 shallow and deep soil moisture for plant production (Fisher et al., 1988; Reynolds et al., 1999;
14 Ogle and Reynolds, 2004). Deep creosotebush roots (70-150 cm depth) may acquire winter-
15 derived soil-water resources that are unavailable to grass species, while active roots near the
16 surface (20-40 cm depth) may serve to access summer-derived shallow soil moisture for plant
17 growth (Gibbens and Lenz, 2001). The observed reduction in summer rain-use efficiency of
18 herbaceous vegetation for the shrub-transition and shrub-dominated landscapes (i.e. variations
19 on the slope of the relationship between herbaceous ANPP and summer precipitation, Fig. 7a)
20 suggests competitive effects of creosotebush for the use of shallow water sources, probably
21 associated to the large spatial extent of near-surface active roots (the radial spread of which
22 typically ranges between 2-6 m, Gibbens and Lenz, 2001). Alternative, landscape changes
23 induced by shrub encroachment (i.e. increased runoff and erosion) may reduce the ability of
24 grass patches to capitalize on horizontal redistribution of runoff for plant growth after summer
25 storms (Wainwright et al., 2000; Turnbull et al., 2012; Stewart et al. 2014).

Deleted: 6

26 Conceptual and mechanistic models of vegetation change suggest that vegetation composition
27 in arid and semi-arid landscapes is likely to be highly sensitive to climate change, and point at
28 variations in the amount and distribution of precipitation as a major driver of shrub
29 encroachment into desert grasslands (Peters, 2002; Gao and Reynolds, 2003; Snyder and
30 Tartowsky, 2006). Overall our results agree with those findings and suggest that changes in
31 the amount and temporal pattern of precipitation comprising reductions in monsoonal summer
32 rainfall and/or increases in winter precipitation may enhance the encroachment of

1 creosotebush into desert grasslands dominated by black and blue grama. Analysis of long-
2 term rainfall series indicates that winter precipitation has increased during the past century in
3 the northern Chihuahuan Desert, particularly since 1950, probably associated with the more
4 frequent occurrence of ENSO events for that period (Dahm and Moore, 1994; Wainwright,
5 2006). This pattern of precipitation change may be responsible, at least in part, of past
6 increase in woody shrub abundance over desert grasslands in the American Southwest (Brown
7 et al., 1997; Snyder and Tartowsky, 2006; Webb et al., 2003). Our results suggest that shrub
8 encroachment has not been particularly active in the studied ecotone for 2000-13 (Fig. 6b).
9 Accordingly, Allen et al. (2008) in a recent study on creosotebush plant architecture and age
10 structure indicated that the most important pulses of shrub encroachment for this area took
11 place between 1950 and 1970. Precise estimation of shrub cover applying segmentation
12 methods in time series of high-resolution imagery could help to accurately determine the
13 intensity of the shrub-encroachment phenomenon under the present variability in precipitation
14 for our grassland-shrubland ecotone.

Deleted: the recent

15 Climate-change projections for the area suggest a general picture of increased aridity in the
16 next 100 years, with increased evaporation due to higher summer temperatures, and increased
17 drought frequency (Christensen and Konikicharla, 2013). The capacity of *L. tridentata* to
18 switch between different soil-water sources (i.e. summer-derived ephemeral shallow soil
19 moisture and more stable deep soil-water reserves derived from winter rainfall) and adapt the
20 timing of vegetation growth to take advantage of changes in resource availability make this C₃
21 shrub less susceptible to predicted increases in aridity than C₄ grasses that are strongly
22 dependent on summer precipitation (Reynolds et al., 1999; Throop et al., 2012; Baez et al.,
23 2013). Current increases in atmospheric CO₂ concentrations may also contribute to reduce the
24 competitiveness of C₄ grasses for the use of soil-water resources against C₃ desert shrubs
25 (Polley et al., 2002). Remaining desert grasslands in the American Southwest may, therefore,
26 be increasingly susceptible to shrub encroachment under the present context of changes in
27 climate and human activities.

28

29 **6 Conclusions**

30 In this study we applied a new analytical methodology for the study of the organization and
31 dynamics of vegetation at a grassland-shrubland Chihuahuan ecotone with variable abundance
32 of grasses (primarily *Boutelua eriopoda* and *B. gracilis*) and shrubs (mainly *Larrea*

Deleted: of analysis

1 *tridentata*), based on the exploration of the relationship between time series of remote-sensed
2 vegetation greenness (NDVI) and precipitation. Our results indicate that the characteristics of
3 the NDVI-rainfall relationships are highly dependent on differences in patterns of water use
4 and plant growth of vegetation types. In fact, NDVI-rainfall relationships show a high
5 sensitivity to spatial variations on dominant vegetation types across the grassland-shrubland
6 ecotone, and provide ready biophysically based criteria to study the spatial distribution and
7 dynamics of net primary production (NPP) for herbaceous and shrub vegetation. The analysis
8 of the relationship between NDVI and precipitation offers, therefore, a powerful methodology
9 for the study of broad-scale vegetation shifts comprising large changes in the dominance of
10 vegetation types in drylands using coarse-grained remotely sensed data, and could be used to
11 target areas for more detailed analysis and/or the application of mitigation measures.

12 Analysis of remote-sensed NPP dynamics at the grassland-shrubland ecotone reflects a
13 variable performance of dominant vegetation types. Herbaceous production is synchronized
14 with monsoonal summer rainfall, while shrub NPP shows a flexible response to both summer
15 and winter precipitation. Overall our results suggest that changes in the amount and temporal
16 pattern of precipitation (i.e. reductions in summer precipitation and/or increases in winter
17 rainfall) may intensify the shrub-encroachment process in the studied desert grasslands of the
18 American Southwest, particularly in the face of predicted general increases in aridity and
19 drought frequency for the area.

20

21 **Acknowledgements**

22 We would like to thank the Sevilleta LTER team, and particularly Scott L. Collins, John
23 Mulhouse and Amaris L. Swann, for logistic support and for granting access to the SEV
24 LTER Five Points NPP and rainfall datasets. We also thank Patricia M. Saco for field
25 assistance. Fieldwork at the Sevilleta National Wildlife Refuge for this study was carried out
26 under permit 22522-14-32, granted by the US Fish and Wildlife Service. An earlier version of
27 this paper benefited from the helpful comments of two anonymous referees. This work is
28 supported by a FP7 Marie Curie IEF fellowship funded by the European Commission (PIEF-
29 GA-2012-329298, VEGDESSERT). Significant funding for collection of the SEV LTER data
30 was provided by the National Science foundation Long Term Ecological Research program
31 (NSF grant numbers BSR 88-11906, DEB 0080529, and DEB 0217774).

32

Deleted: -

Deleted: pattern

1 **References**

2 Al-Bakri, J. T., and Suleiman, A. S.: NDVI response to rainfall in different ecological zones
3 in Jordan, *Int. J. Remote Sens.*, 10, 3897-3912, 2004.

4 [Allen, A. P., Pockman, W. T., Restrepo, C., and Milne, B. T.: Allometry, growth and](#)
5 [population regulation of the desert shrub Larrea tridentata, *Funct. Ecol.*, 22, 197-204, 2008.](#)

6 Anderson, G. L., Hanson, J. D., and Haas., R. H.: Evaluating Landsat Thematic Mapper derived
7 vegetation indices for estimating above-ground biomass on semiarid rangelands, *Remote Sens.*
8 *Environ.*, 45, 165-175, 1993.

9 Baez, S., Collins, S. C., Pockman, W. T., Johnson, J. E., and Small, E. E.: Effects of
10 experimental rainfall manipulations on Chihuahuan Desert grassland and shrubland plant
11 communities, *Oecologia*, 172, 1117-1127, 2013.

12 Brown, J. H., Valone, T. J., and Curtin, C. G.: Reorganization of an arid ecosystem in response
13 to recent climate change, *P. Natl. Acad. Sci. USA.*, 94, 9729-9733, 1997.

14 Buffington, L. C., and Herbel, C. H.: Vegetational changes on a semidesert grassland range
15 from 1858 to 1963, *Ecol. Monogr.*, 35, 139-164, 1965.

16 [Carlson, T. N., and Ripley, D. A.: On the relation between NDVI, fractional cover, and leaf](#)
17 [area index, *Remote Sens. Environ.*, 62, 241-252, 1997.](#)

18 Choler, P., Sea, W., Briggs, P., Raupauch, M., and Leuning, R.: A simple ecohydrological
19 model captures essentials of seasonal leaf dynamics in semiarid tropical grasslands,
20 *Biogeosciences*, 7, 907-920, 2010.

21 Christensen, J. H, and Konikicharla, K. K.: Climate phenomena and their relevance for future
22 regional climate change, in: *Climate Change 2013: The Physical Science Basis, Contribution of*
23 *Working Group I to the Fifth Assessment Report of the Intergovernmental Panel on Climate*
24 *Change*, edited by: Stoker, T. F., Qin, D., Platter, G. K., Tignor, M., Allen, S. K., Boschung, J.,
25 Navels, A., Xia, Y., Bex, V., and Midgley, P. M., Cambridge University Press, Cambridge, UK,
26 1217-1308, 2013.

27 [Collins, S. L., Belnap, J., Grimm, N. B., Rudgers, J. A., Dahm, C. N., D'Odorico, P., Litvak,](#)
28 [M., Natvig, D. O., Peters, D. C., Pockman, W. T., Sinsabaugh, R. L., and Wolf, B. O.: A](#)
29 [multiple, hierarchical model of pulse dynamics in arid-land ecosystems, *Annu. Rev. Ecol. Evol.*](#)
30 [Syst., 45, 397-419, 2014.](#)

1 [Dahm, C. N., and Moore, D. I.: The El Niño/Southern Oscillation phenomenon and the](#)
2 [Sevilleta Long-Term Ecological Research site, in: El Niño and Long-Term Ecological Research](#)
3 [\(LTER\) Sites, edited by: Greenland, D., LTER Network Office, University of Washington,](#)
4 [Seattle, USA, 12-20, 1994.](#)

5 [DeFries, R. S., Hansen, M. C., and Townshend, J. R.G.: Global continuous fields of vegetation](#)
6 [characteristics: a linear mixture model applied to multiyear 8 km AVHRR data, Int. J. Remote](#)
7 [Sens., 21, 1389-1414, 2000.](#)

8 D'Odorico, P., Okin, G. S., and Bestelmeyer, B. T.: A synthetic review of feedbacks and
9 drivers of shrub encroachment in arid grasslands, *Ecohydrology*, 5, 520-530, 2012.

10 Evans, J., and Geerken, R.: Discrimination between climate and human-induced dryland
11 degradation, *J. Arid Environ.*, 57, 535-554, 2004.

12 Fisher, F. M., Zak, J. C., Cunningham, G. L., and Whitford, W. G.: Water and nitrogen effects
13 on growth and allocation patterns of creosotebush in the northern Chihuahuan Desert, *J. Range*
14 *Manage.*, 41, 387-391, 1988.

15 Forzieri, G., Castelli, F., and Vivoni, E. R.: Vegetation dynamics within the North American
16 Monsoon Region, *J. Climate*, 24, 1763-83, 2011.

17 Gao, Q., and Reynolds, J. F.: Historical shrub-grass transitions in the northern Chihuahuan
18 Desert: Modeling the effects of shifting rainfall seasonality and event size over a landscape,
19 *Global Change Biol.*, 9, 1-19, 2003.

20 Garcia, M., Litago, J., Palacios-Orueta, A., Pinzon, J. E., and Ustin, S. L.: Short-term
21 propagation of rainfall perturbations on terrestrial ecosystems in central California, *Appl. Veg.*
22 *Sci.*, 13, 146-162, 2010.

23 Gibbens, R. P., and Lenz, J. M.: Root systems of some Chihuahuan Desert plants, *J. Arid*
24 *Environ.*, 49, 221-263, 2001.

25 Gilad, E., Shachak, M., and Meron, E.: Dynamics and spatial organization of plant
26 communities in water-limited systems, *Theor. Popul. Biol.*, 72, 214-230, 2007.

27 [Girden, E. R.: ANOVA: repeated measures, SAGE University Paper Series 7-84, SAGE](#)
28 [Publications, Newbury Park, USA, 1992.](#)

1 Godin-Alvarez, H., Herrick, J. E., Mattocks, M., Toledo, D., and Van Zee, J.: Comparison of
2 three vegetation monitoring methods: their relative utility for ecological assessment and
3 monitoring, *Ecol. Indic.*, 9, 1001-1008, 2009.

4 Gosz, J. R.: Ecological functions in a biome transition zone: translating local responses to
5 broad-scale dynamics, in: *Landscape Boundaries: Consequences for Biotic Diversity and*
6 *Ecological Flows*, edited by: Hansen, A. J., and di Castri, A. J., Springer, New York, USA, 56-
7 75, 1992.

8 Hansen, M. C., Defries, R. S., Townshend, J. R. G., Sohlberg, R., Dimiceli, C., and Carroll,
9 M.: Towards an operational MODIS continuous field of percent tree cover algorithm: examples
10 using AVHRR and MODIS data, *Remote Sens. Environ.*, 83, 303-319, 2002.

11 Hochstrasser, T., Kroel-Dulay, G., Peters, D. P., and Gosz, J. R.: Vegetation and climate
12 characteristics of arid and semi-arid grasslands in North America and their biome transition
13 zone, *J. Arid Environ.*, 51, 55-78, 2002.

14 Holm, A. McR., Cridland, S. W., and Roderick, M. L.: The use of time-integrated NOAA
15 NDVI data and rainfall to assess landscape degradation in the arid and shrubland of Western
16 Australia, *Remote Sens. Environ.*, 85, 145-158, 2003.

17 Huenneke, L. F., Anderson, J. P., Remmenga, M., and Schlesinger, W. H.: Desertification alters
18 patterns of aboveground net primary production in Chihuahuan ecosystems, *Global Change*
19 *Biol.*, 8, 247-264, 2002.

20 Huete, A., Jackson, R. D., and Post, D. F.: Spectral response of a plant canopy with different
21 soil backgrounds, *Remote Sens. Environ.*, 17, 37-53, 1985.

22 Huete, A., Didan, K., Miura, T., Rodriguez, E. P., Gao, X., and Ferreira, L. G.: Overview of the
23 radiometric and biophysical performance of the MODIS vegetation indices, *Remote Sens.*
24 *Environ.*, 83, 195-213, 2002.

25 Lu, H., Raupach, M. R., McVicar, T. R., and Barret, D. J.: Decomposition of vegetation cover
26 into woody and herbaceous components using AVHRR NDVI time series, *Remote Sens.*
27 *Environ.*, 86, 1-16, 2003.

28 Millennium Ecosystem Assessment: *Ecosystems and Human Well-being: Biodiversity*
29 *Synthesis*, World Resources Institute, Washington, DC, USA, 2005.

1 Montandon, L. M., and Small, E. E.: The impact of soil reflectance on the quantification of the
2 green vegetation fraction from NDVI, *Remote Sens. Environ.*, 112, 1835-1845, 2008.

3 Moreno-de las Heras, M., Saco, P. M., Willgoose, G. R., and Tongway, D. J.: Variations in
4 hydrological connectivity of Australian semiarid landscapes indicate abrupt changes in rainfall-
5 use efficiency of vegetation, *J. Geophys. Res.*, 117, G03009, doi:10.1029/2011JG001839, 2012.

6 Mueller E. N., Wainwright, J., and Parsons, A. J.: The stability of vegetation boundaries and
7 the propagation of desertification in the American Southwest: A modelling approach, *Ecol.*
8 *Model.*, 208, 91-101, 2007.

9 Muldavin, E. H., Moore, D. I., Collins, S. L., Wetherill, K. R., and Lightfoot, D. C.:
10 Aboveground net primary production dynamics in a northern Chihuahuan Desert ecosystem,
11 *Oecologia*, 155, 123-132, 2008.

12 Munkhtsetseg, E., Kimura, R., Wand, J., and Shinoda, M.: Pasture yield response to
13 precipitation and high temperature in Mongolia, *J. Arid Environ.*, 70, 1552-1563, 2007.

14 Notaro, M., Liu, Z., Gallimore, R. G., Williams, J. W., Gutzler, D. S., and Collins, S.: Complex
15 seasonal cycle of ecohydrology in the Southwest United States, *J. Geophys. Res.*, 115, G04034,
16 doi: 10.1029/2010JG001382, 2010.

17 Ogle, K., and Reynolds, J. F.: Plant responses to precipitation in desert ecosystems: integrating
18 functional types, pulses, thresholds and delays, *Oecologia*, 141, 282-294, 2004.

19 Okin, G. S., and Roberts, D.A.: Remote sensing in arid environments: challenges and
20 opportunities, in: *Manual of Remote Sensing Vol 4: Remote Sensing for Natural Resource*
21 *Management and Environmental Monitoring*, edited by: Ustin, S., John Wiley and Sons, New
22 York, USA, 111-146, 2004.

23 Okin, G. S., Roberts, D. A., Murray, B., and Okin, W. J.: Practical limits on hyperspectral
24 vegetation discrimination in arid and semiarid environments, *Remote Sens. Environ.*, 77, 212-
25 225, 2001.

26 Okin, G. S., Parsons, A. J., Wainwright, J., Herrick, J. E., Bestelmeyer, B. T., Peters, D. C., and
27 Fredrickson, E. L.: Do changes in connectivity explain desertification? *BioScience*, 59, 237-
28 244, 2009.

29 Pennington, D. D., and Collins, S. L.: Response of an aridland ecosystem to interannual climate
30 variability and prolonged drought, *Landscape Ecology*, 22, 897-910, 2007.

1 Peters, D. P. C.: Plant species dominance at a grassland-shrubland ecotone: and individual-
2 based gap dynamics model of herbaceous and woody species, *Ecol. Model.*, 152, 5-32, 2002.

3 Peters, A. J., and Eve, M. D.: Satellite monitoring of desert plant community response to
4 moisture availability, *Environ. Monit. Assess.*, 37, 273-287, 1995.

5 Peters, A. J., Eve, M. D., Holt, E. H., and Whitford, W. G.: Analysis of desert plant community
6 growth patterns with high temporal resolution satellite spectra, *J. Appl. Ecol.*, 34, 418-432,
7 1997.

8 Petrie, M. D., Collins, S. L., Gutzler, D. S., and Moore, D. M.: Regional trends and local
9 variability in monsoon precipitation in the northern Chihuahuan desert, USA, *J. Arid Environ.*,
10 103, 63-70, 2014.

11 Pockman, W. T., and Small, E. E.: The influence of spatial patterns of soil moisture on the
12 grass and shrub responses to a summer rainstorm in a Chihuahuan desert ecotone, *Ecosystems*,
13 13, 511-525, 2010.

14 Polley, H. W., Johnson, H. B., and Tischler, C. R.: Woody invasion of grasslands: evidence that
15 CO₂ enrichment indirectly promotes establishment of *Prosopis glandulosa*, *Plant Ecol.*, 164,
16 85-94, 2002.

17 Prasad, V. K., Badarinath, K. V. S., and Eaturu, A.: Spatial patterns of vegetation phenology
18 metrics and related climatic controls of eight contrasting forest types in India-analysis from
19 remote sensing datasets, *Theor Appl Climatol*, 89, 95-107, 2007.

20 Ravi, S, Breshears, D. D., Huxman, T. E., and D'Odorico, P.: Land degradation in drylands:
21 Interactions among hydrologic-aeolian processes and vegetation dynamics, *Geomorphology*,
22 116, 236-245, 2010.

23 Reynolds, J. F., Virginia, R. A., Kemp, P. R., de Soyza, A. G., and Tremmel, D. C.: Impact of
24 drought on desert shrubs: effects of seasonality and degree of resource island development,
25 *Ecol. Monogr.*, 69, 69-106, 1999.

26 Reynolds, J. F., Kemp, P. R., Ogle, K., and Fernandez, R. J.: Modifying the 'pulse-reserve'
27 paradigm for deserts of North America: precipitation pulses, soil water, and plant responses,
28 Oecologia, 141, 194-210, 2004.

1 Rietkerk, M., Boerlijst, M. C., Van Langevelde, F., HilleRisLambers, R., Van de Koppel, J.,
2 Kumar, L., Prins, H. H. T., and de Roos, A. M.: Self-organization of vegetation in arid
3 ecosystems, *Am. Nat.*, 160, 524-530, 2002.

4 [Roderick, M. L., Noble, I. R., and Cridland, S. W.: Estimating woody and herbaceous cover](#)
5 [from time series satellite observations, Global Ecol. Biogeogr., 8, 501-508, 1999.](#)

6 Saco, P. M., and Moreno-de las Heras, M.: Ecogeomorphic coevolution of semiarid hillslopes:
7 emergence of banded and striped vegetation patterns through interaction of biotic and abiotic
8 processes, *Water Resour. Res.*, 49, 115-126, 2013.

9 Schwinnig, S. and Sala, O.E.: Hierarchy of responses to resource pulses in arid and semi-arid
10 ecosystems, *Oecologia*, 141, 211-220, 2004.

11 Schlesinger, W. H., Reynolds, J. F., Cunningham, G. L., Huenneke, L. F., Jarrell, W. M.,
12 Virginia, R. A., and Whittford, W. G.: Biological feedbacks in global desertification, *Science*,
13 247, 1043-1048, 1990.

14 Smith, M. O., Ustin, S. L., Adams, J. B., and Gillespie, A. R.: Vegetation in deserts: I. a
15 regional measure of abundance from multispectral images, *Remote Sens. Environ.*, 31, 1-26,
16 1990.

17 Snyder, K. A., and Tartowsky, S. L.: Multi-scale temporal variation in water availability:
18 Implications for vegetation dynamics in arid and semi-arid ecosystems, *J. Arid Environ.*, 65,
19 219-234, 2006.

20 Soil Survey Staff: *Keys to Soil Taxonomy*, 11th Ed., USDA Natural Resources Conservation
21 Service, Washington, USA, 2010.

22 Somers, B., Asner, G. P., Tits, L., and Coppin, P.: Endmember variability in Spectral Mixture
23 Analysis: A review, *Remote Sens. Environ.*, 115, 1603-1616, 2011.

24 Sparrow, A. D., Friedel, M. H., Stafford-Smith, D. M.: A landscape-scale model of shrub and
25 herbage dynamics in Central Australia, validated by satellite data, *Ecol. Model.*, 97, 197-213,
26 1997.

27 Stewart, J., Parsons, A. J., Wainwright, J., Okin, G. S., Bestelmeyer, B. T., Fredrickson, E. L.,
28 and Schlesinger, W. H.: Modelling emergent patterns of dynamic desert ecosystems, *Ecol.*
29 *Monogr.*, 84, 373-410, 2014.

1 Throop, H. L., Reichman, L. G., and Archer, S. R.: Response of dominant grass and shrub
2 species to water manipulation: an ecophysiological basis for shrub invasion in a Chihuahuan
3 Desert grassland, *Oecologia*, 169, 373-383, 2012.

4 Turnbull, L., Brazier, R. E., Wainwright, J., Dixon, L., and Bol, R.: Use of carbon isotope
5 analysis to understand semi-arid erosion dynamics and long-term semi-arid degradation, *Rapid*
6 *Commun. Mass Sp.*, 22, 1697-1702, 2008.

7 Turnbull, L., Wainwright, J., and Brazier, R. E.: Changes in hydrology and erosion over a
8 transition from grassland to shrubland, *Hydrol. Process.*, 24, 393-414, [2010a](#). Deleted: 2010b

9 Turnbull, L., Wainwright, J., Brazier, R. E., and Bol, R.: Biotic and abiotic changes in
10 ecosystem structure over a shrub-encroachment gradient in the southwestern USA, *Ecosystems*,
11 13, 1239-1255, [2010b](#). Deleted: 2010a

12 Turnbull, L., Wainwright, J. and Ravi, S.: Vegetation change in the southwestern USA: patterns
13 and processes, in: *Patterns of Land Degradation in Drylands, Understanding Self-Organised*
14 *Ecogeomorphic Systems*, edited by: Mueller, E. N., Wainwright, J., Parsons, A. J., and
15 Turnbull, L., Springer, New York, USA, 289-313, 2014.

16 Turnbull, L., Wilcox, B. P. , Belnap, J., Ravi, S., D'Odorico, P., Childers, D. L., Gwenzi, W.,
17 Okin, G. S., Wainwright, J., Caylor, K. K., and Sankey T.: Understanding the role of
18 ecohydrological feedbacks in ecosystem state change in drylands, *Ecohydrology*, 5, 174-183,
19 2012.

20 Turnbull, L., Parsons, A. J., Wainwright, J., and Anderson, J. P.: Runoff responses to long-term
21 rainfall variability in a shrub-dominated catchment, *J. Arid Environ.*, 91, 88-94, 2013.

22 van Auken, O. W.: Shrub invasions of North American semiarid grasslands, *Annu. Rev. Ecol.*
23 *Syst.*, 12, 352-356, 2000.

24 Veron, S. R., and Paruelo, V.: Desertification alters the response of vegetation to changes in
25 precipitation, *J. App. Ecol.*, 47, 1233-1241, 2010.

26 Wainwright, J.: Climate and climatological variations in the Jornada Range and neighboring
27 areas of the US South West, *Advances in Environmental Monitoring and Modelling*, 1, 39-110,
28 2005.

1 Wainwright, J., Parsons, A. J., and Abrahams, A. D.: Plot-scale studies of vegetation, overland
2 flow and erosion interactions: case studies from Arizona and New Mexico, *Hydrol. Process.*,
3 14, 2921-2943, 2000.

4 Webb, R. H., Turner, R. M., Bowers, J. E., and Hastings, J. R.: The Changing Mile Revisited.
5 An Ecological Study of Vegetation Change with Time in the Lower Mile of an Arid and
6 Semiarid Region, University of Arizona, Tucson, USA, 2003.

7 Weiss, J. L., Gutzler, D. S., Coonrod, J. E. A., and Dahm, C. N.: Long-term vegetation
8 monitoring with NDVI in a diverse semi-arid setting, central New Mexico, USA, *J. Arid
9 Environ.*, 58, 249-272, 2004.

10

1 **Table 1.** Main effects and interactions of seasonal precipitation (preceding non-monsoonal
 2 rainfall, October-May; monsoonal summer rainfall, June-September; late non-monsoonal
 3 rainfall, October-March) and landscape type (4 levels: grass-dominated, grass-transition,
 4 shrub-transition, and shrub-dominated landscapes) on remote-sensing estimated annual (per
 5 growing cycle, April-March) net primary production for herbaceous vegetation and shrubs.

	<i>F</i>	df	<i>P</i>	η^2 (%)
Herbaceous vegetation ANPP _{r.sensing}				
Rain _{PNM} (Oct-May)	194.2	1	0.000	4.2
Rain _{SM} (June-Sept.)	1483.4	1	0.000	25.4
Rain _{LNM} (Oct.-March)	129.3	1	0.000	2.0
LT	35.9	3	0.000	2.3
LT:Rain _{PNM} (Oct-May)	122.4	3	0.000	7.8
LT:Rain _{SM} (June-Sept.)	282.4	3	0.000	16.2
LT:Rain _{LNM} (Oct.-March)	1.1	3	0.326	0.0
Shrubs ANPP _{r.sensing}				
Rain _{PNM} (Oct-May)	1661.2	1	0.000	27.7
Rain _{SM} (June-Sept.)	1720.8	1	0.000	28.4
Rain _{LNM} (Oct.-March)	7.1	1	0.010	0.1
LT	2.9	3	0.030	0.2
LT:Rain _{PNM} (Oct-May)	6.6	3	0.000	0.4
LT:Rain _{SM} (June-Sept.)	46.2	3	0.000	3.0
LT:Rain _{LNM} (Oct.-March)	31.9	3	0.000	2.1

6 Abbreviations: ANPP_{r.sensing}, remote-sensed annual net primary production; Rain_{PNM} (Oct-May),
 7 preceding non-monsoonal rainfall; Rain_{SM} (June-Sept.), monsoonal summer rainfall; Rain_{LNM} (Oct.-
 8 March), late non-monsoonal rainfall; LT, landscape type; ‘:’, interaction terms; η^2 , eta-squared
 9 (effect size).

10 Notes: η^2 values in bold are > 10% (effects that contribute in more than 10% to the total
 11 variance comprised in ANPP_{r.sensing}).

1 **Fig. 1.** Simulated dryland biomass-rainfall relationships for herbaceous and shrub vegetation:
2 (a) modelled biomass dynamics for an herbaceous (green) and a shrub (red) species, (b) strength of the biomass-precipitation relationship (Pearson's R correlation) using different
3 lengths of rainfall accumulation for the simulated herbaceous and shrub species (values above
4 the dotted grey line are significant at $P<0.05$), (c) optimal rainfall accumulation length (Olr)
5 as a function of the plant-growth and mortality rates. $ARain_{hv}$ and $ARain_s$ lines in panel (a)
6 represent the antecedent rainfall series that best correlate with the simulated series of
7 herbaceous and shrub biomass, respectively (i.e. time series of precedent rainfall with rainfall
8 accumulation lengths Olr_{hv} for herbaceous vegetation and Olr_s for shrubs). The green and red
9 dots in panel (c) indicate optimal rainfall accumulation lengths obtained for the simulated
10 herbaceous (Olr_{hv} , 52 days) and shrub (Olr_s , 104 days) species, respectively. The (grey)
11 "vegetation extinction" area in panel (c) reflects combined values of plant-growth and
12 mortality rates that do not support long-term vegetation dynamics for the simulated rainfall
13 conditions.
14

15
16 **Fig. 2.** Study area: (a) location of the Sevilleta National Wildlife Refuge (SNWR) and
17 distribution of major New Mexico biomes, (b) regional location of the study area (McKenzie
18 Flats, SNWR), (c) detailed location of the study site (18-km² area) and general view of the
19 reference SEV LTER Black Grama (right) and Creosotebush (left) Core Sites. Map (a)
20 follows the Sevilleta LTER classification of New Mexico biomes (Sevilleta LTER,
21 <http://sev.lternet.edu/content/new-mexico-biomes-created-sevlter>). Source for background
22 image in panels (b) and (c): 2009 National Aerial Imagery Program (USDA Farm Service
23 Agency).
24

25 **Fig. 3.** Reference NDVI-rainfall relationships at the SEV LTER Black Grama and
26 Creosotebush Core Sites: (a) 2000-13 MODIS NDVI time series for the Core Sites, (b)
27 strength of the NDVI-rainfall relationship (Pearson's R correlation) for the Core Sites using
28 different lengths of rainfall accumulation (maximum correlations, R_{max} , for the annual cycles
29 of vegetation growth are shown together with the 2000-13 mean trend; detailed correlograms
30 for each growing cycle can be found in Supplementary Fig. 1 as online supporting
31 information for this study). R values above the dotted grey line are significant at $P<0.05$.
32 $ARain_{hv}$ and $ARain_s$ lines in panel (a) represent the antecedent rainfall series that best correlate

Deleted: A
Deleted: B
Deleted: (RaL)
Deleted: C
Deleted: plant biomass-rainfall signature
Deleted: (RaL_{max}, length of rainfall accumulation that maximizes the plant biomass-precipitation relationship)

Deleted: C
Deleted: RaL_{max}
Deleted: values
Deleted:
Deleted: C

Deleted: A
Deleted: B
Deleted: C
Deleted: A
Deleted: B
Deleted: C

Deleted: A
Deleted: c
Deleted: s
Deleted: B
Deleted: c
Deleted: s
Deleted: individual
Deleted: growing

1 with the NDVI series for the Black Grama and Creosotebush Core sites (i.e. time series of
2 precedent rainfall with rainfall accumulation lengths Olr_{hv} for herbaceous vegetation and Olr_s
3 for shrubs). Reference Olr_{hv} and Olr_s values in panel (b) represent the optimal rainfall
4 accumulation lengths for herbaceous vegetation (57 days) and shrubs (145 days), respectively.

Deleted: B
Deleted: indicate
Deleted: reference NDVI-rainfall signatures
Deleted: of the antecedent rainfall series that maximize the relationships between NDVI and precipitation

5
6 **Fig. 4.** Principal Component Analysis (PCA) of the NDVI-rainfall correlation coefficients for
7 the herbaceous- and shrub-specific antecedent rainfall series $ARain_{hv}$ and $ARain_s$ (57- and
8 145-day cumulative rainfall series, respectively) and resulting landscape type classification
9 across the 18 km² study area: (a) PCA projection of cases (MODIS pixels), (b) PCA
10 projection of variables (per growing cycle NDVI-antecedent rainfall correlation scores), (c)
11 landscape type classification (GD, grass-dominated, GT, grass-transition, ST, shrub-
12 transition, and SD, shrub-dominated landscapes) as a function of the relationship between
13 PCA Factor 1 and field-estimated vegetation dominance for a reference set of 27 control
14 points, (d) spatial distribution of landscape types in the study area, (e) general view and
15 characteristics of the landscape types. MODIS pixel locations for the ground control points
16 are highlighted in panel (a). Vector labels in panel (b) indicate the dates of the yearly cycles
17 of vegetation growth (April-March). Source for background image in panel (d): 2009 National
18 Aerial Imagery Program (USDA Farm Service Agency).

Deleted: A
Deleted: B
Deleted: C
Deleted: D
Deleted: E
Deleted: A
Deleted: B
Deleted: D

19
20 **Fig. 5.** NDVI decomposition and transformation into partial Annual Net Primary Production
21 (ANPP) components for herbaceous and shrub vegetation: (a) decomposed NDVI time series
22 of herbaceous and shrub vegetation for the reference SEV LTER Black Grama and
23 Creosotebush Core Sites, (b) relationships between field ANPP and the (per growing cycle)
24 annual integrals of herbaceous and shrub NDVI components for the SEV LTER Core Sites,
25 (c) remote-sensed ANPP estimates against field ANPP determinations (root mean square
26 error, RMSE, and normalized error, NRMSE, of the estimates are shown within the plot) (d)
27 remote-sensed ANPP estimations of herbaceous and shrub vegetation (mean for the 2000-13
28 series), and (e) herbaceous and shrub contribution to total ANPP (mean for the 2000-13
29 series) across the 18-km² study area.

Deleted: A
Deleted: B
Deleted: c
Deleted: s
Deleted: C
Deleted: D

1 [Fig. 6. Spatiotemporal dynamics of remote-sensed ANPP: \(a\) ANPP differences between](#)
2 [landscape types \(grass-dominated, grass-transition, shrub-transition, and shrub-dominated](#)
3 [landscapes\) along 2000-13, \(b\) 2000-13 temporal variations of the shrub contribution to total](#)
4 [ANPP for the different landscape types \(Pearson's \$R\$ correlations of shrub ANPP contributions](#)
5 [with time\). Different letters in panel \(a\) for each cycle of vegetation growth indicate](#)
6 [significant differences between landscape types at \$P<0.05\$ \(tested using repeated-measures](#)
7 [ANOVA and post-hoc Tukey HSD tests\). Dotted lines in panel \(b\) represent weak \(\$R<0.40\$ \)](#)
8 [correlations. Displayed correlations are significant at \$P<0.05\$. Numbers in plot \(c\) indicate](#)
9 [correlation coefficients.](#)

10

11 **Fig. 7.** Scatter plots and correlations (Pearson's R) between remote-sensed ANPP
12 estimations and seasonal precipitation (preceding non-monsoonal, summer monsoonal, and
13 late non-monsoonal rainfall) for the different landscape types (grass-dominated, grass-
14 transition, shrub-transition, and shrub-dominated landscapes): (a) herbaceous ANPP, (b)
15 shrub ANPP. Solid and dotted lines represent strong ($R \geq 0.40$) and weak ($R < 0.40$)
16 correlations, respectively. Displayed correlations are significant at $P<0.05$. Numbers within
17 the plots indicate correlation coefficients.

Deleted: A
Deleted: B
Deleted: , $P<0.01$
Deleted: , $P<0.05$

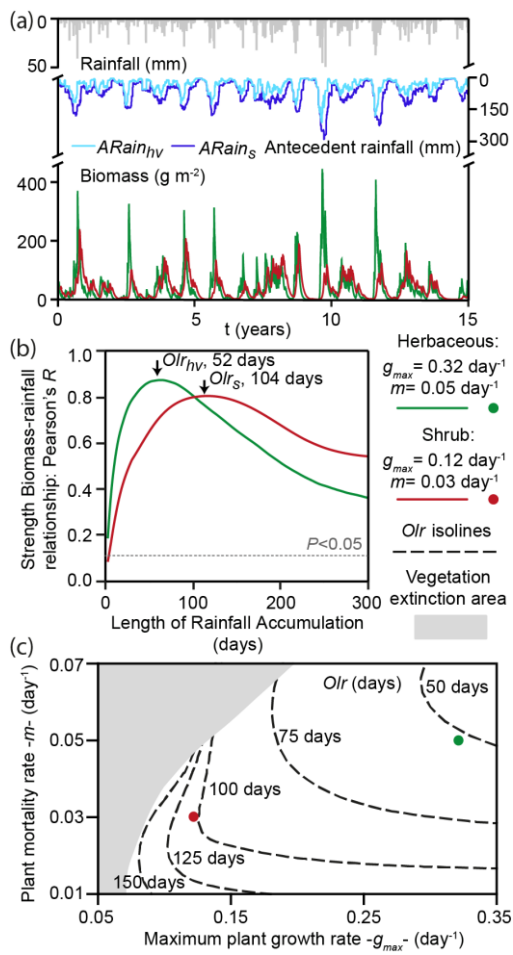


Fig. 1.

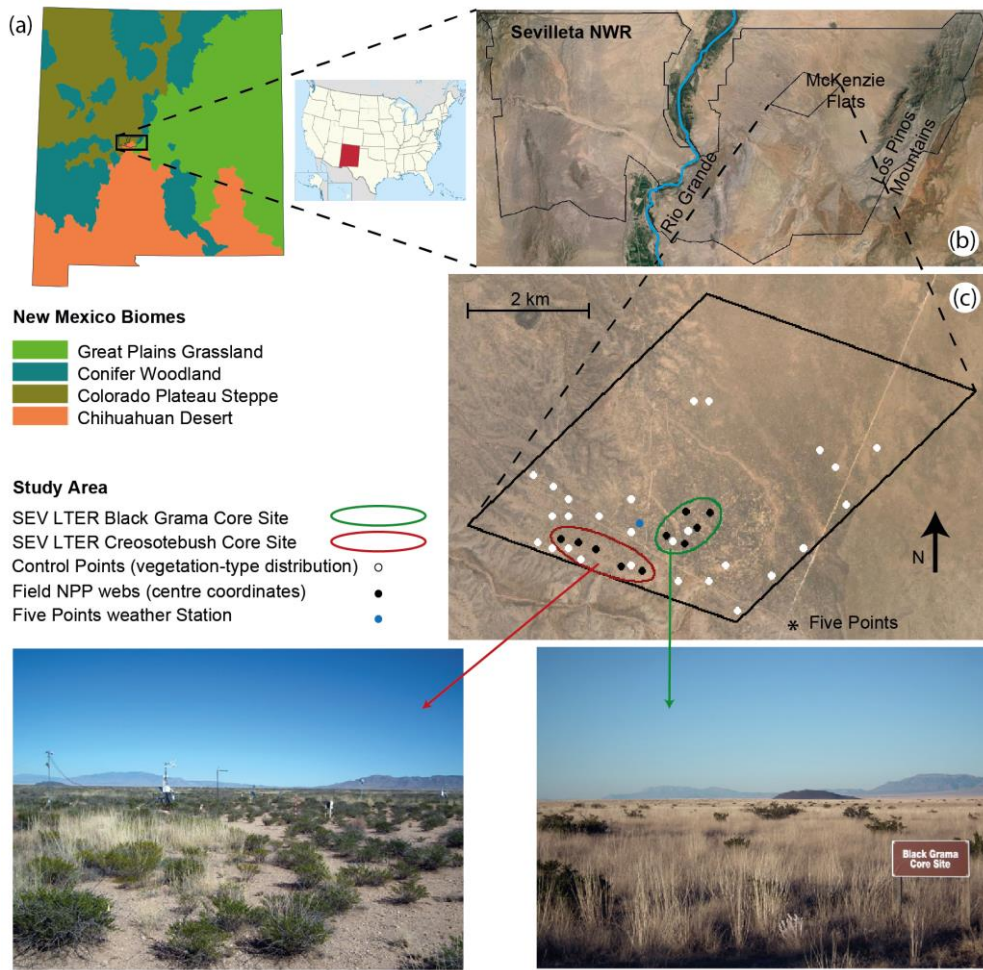


Fig. 2.

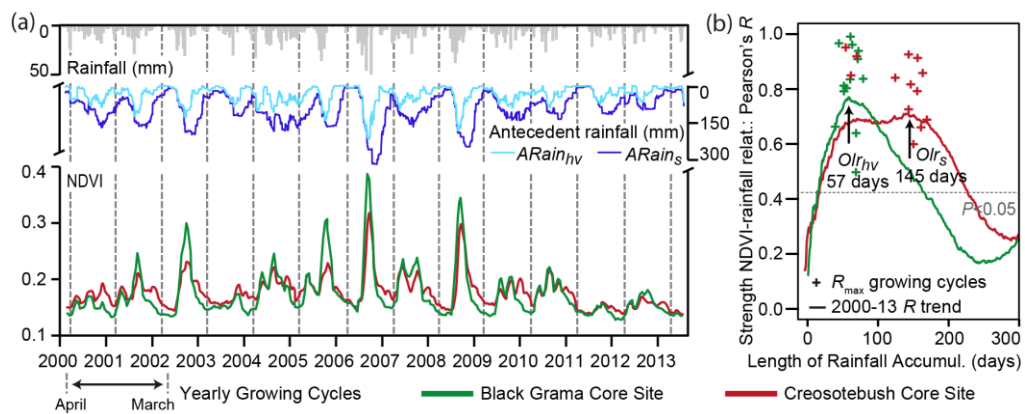


Fig. 3.

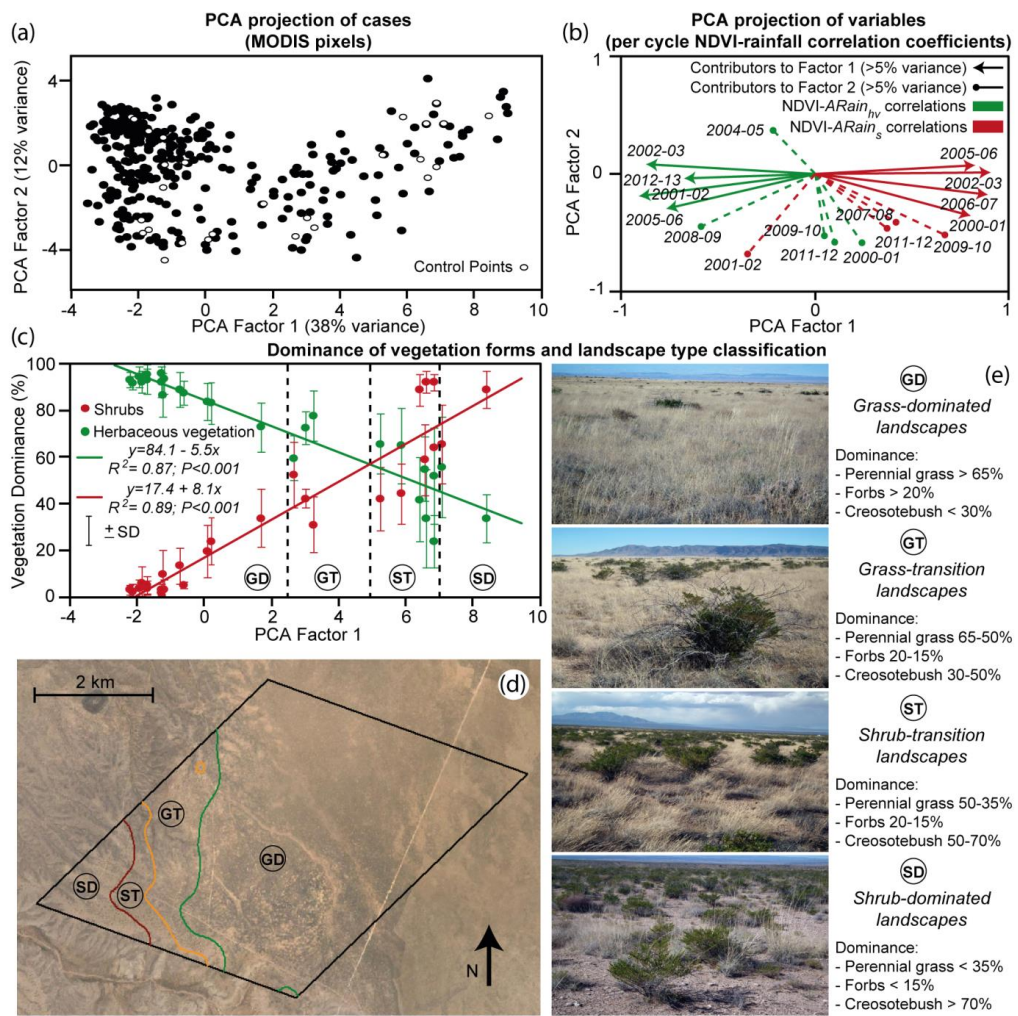


Fig. 4.

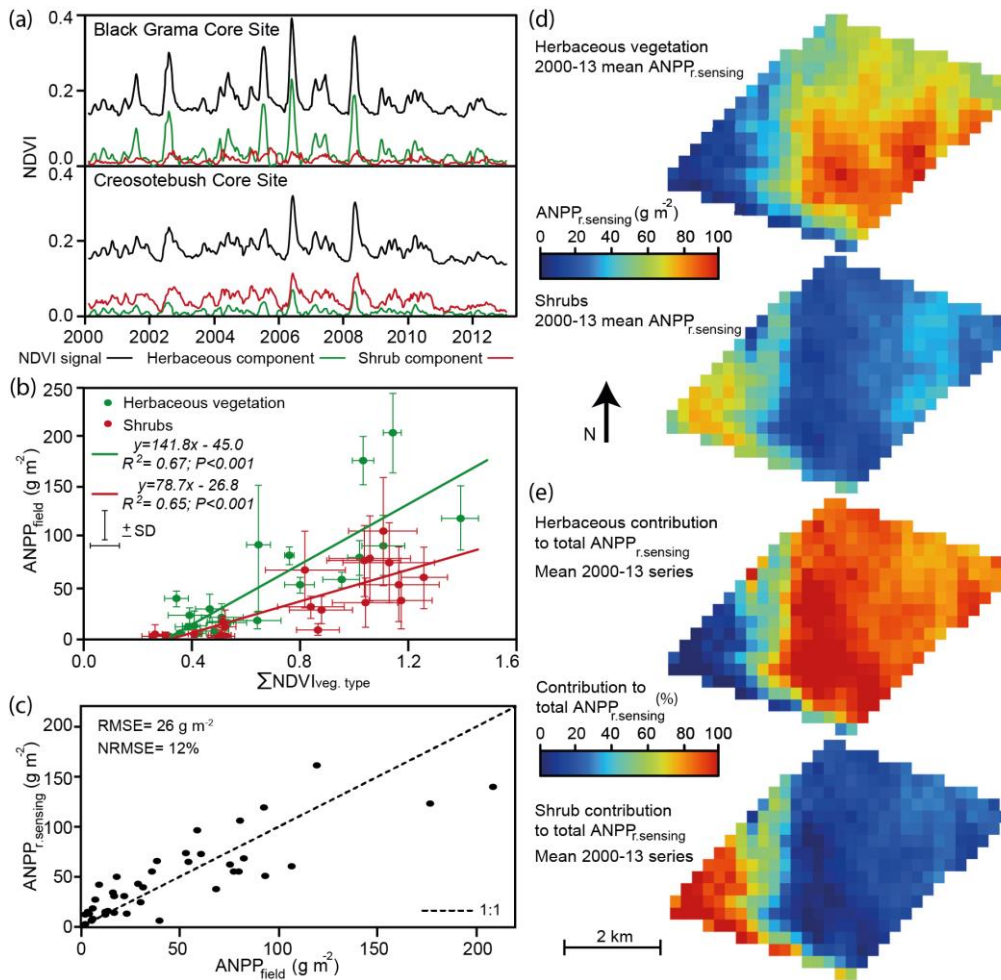


Fig. 5.

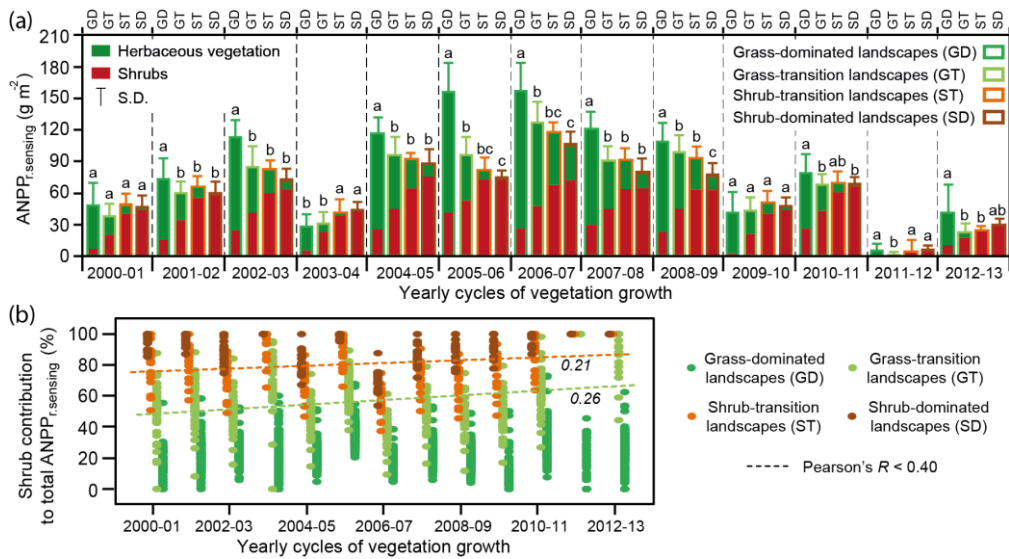
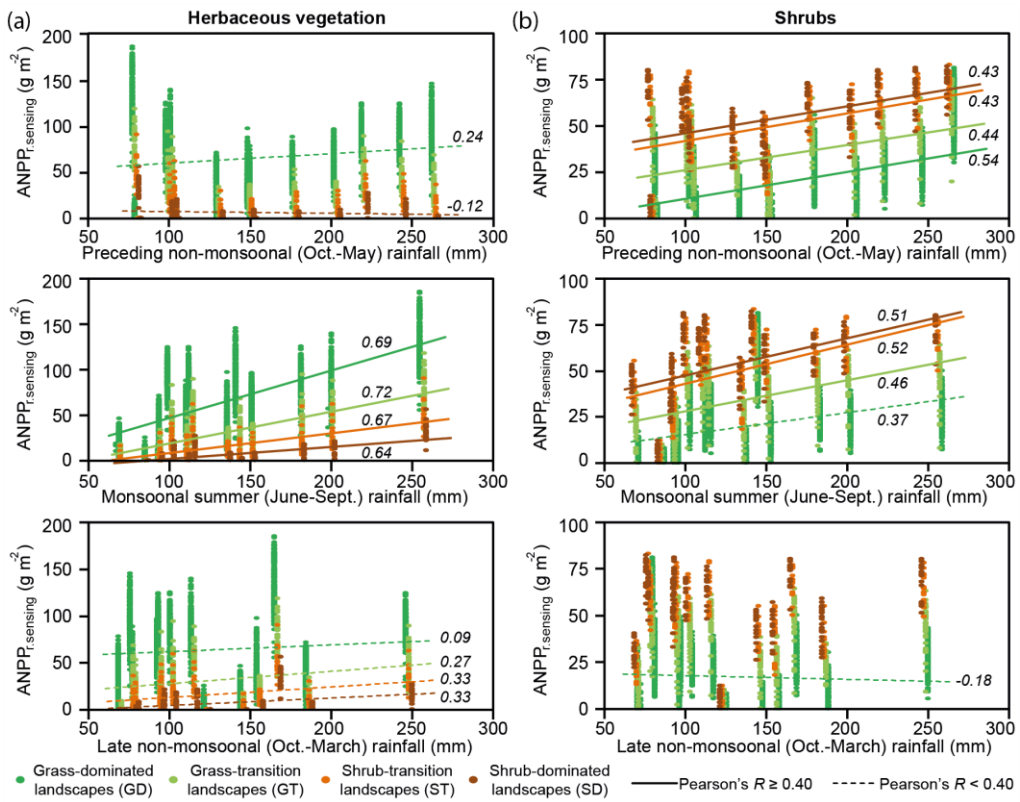


Fig. 6.

1



1 In this document we provide the Maple 9.5 (Maplesoft, Waterloo, Canada) codes used in the
2 paper (Code 1) to simulate dryland biomass dynamics for an herbaceous and a shrub species,
3 and (Code 2) to decompose single time series of NDVI into partial components for
4 herbaceous and shrub vegetation applying the reference vegetation-type characteristic
5 antecedent rainfall series for herbs and shrubs ($ARain_{hv}$ and $ARain_s$, respectively). We also
6 provide two supplementary figures: (i) Supplementary Fig. 1 that presents the results of our
7 model sensitivity analysis, and (ii) Supplementary Fig. 2 that presents detailed NDVI-
8 antecedent rainfall correlograms obtained for each growing cycle of vegetation growth (April-
9 March) in the reference Black Grama and Creosotebush SEV LTER Core Sites.

10

11

12

13

14 Contents:

15 Code 1.....	Page 2
16 Code 2.....	Page 6
17 Supplementary Fig. 1.....	Page 10
18 <u>Supplementary Fig. 2</u>	<u>Page 11</u>

19

Deleted: a
Deleted: (

Deleted:)

```

1  Code 1: Dynamic Vegetation Model
2
3  Input files (location: C:\DataFolder\):
4  1. Daily rainfall: Rain.txt
5  Data is stored in columns 1 and 2 for dates and rainfall, respectively.
6
7  Output files (location: C:\DataFolder\):
8  1. Temporal series of herbaceous and shrub biomass: Biomass.txt
9  Data is stored in columns 1, 2 and 3 for dates, herbaceous and shrub biomass, respectively.
10 2. Temporal series of herbaceous and shrub biomass graph: Biomass.png (green, herbaceous
11 biomass; red, shrub biomass; blue, daily rainfall).
12
13 Procedure:
14 1. We load the Maple packages required for the subsequent calculations.
15  > with(linalg): with(plots): with(LinearAlgebra): with(Statistics): with(plottools):
16
17 2. We load the daily rainfall data file.
18  > droot := "C:\\DataFolder\\":
19  drain := ImportMatrix(cat(droot, "Rain.txt"), source = delimited, delimiter = " ", datatype
20 = anything):
21  dates := ImportMatrix(cat(droot, "Rain.txt"), source = delimited, delimiter = "", ,
22 datatype=string):
23
24 3. We define a rainfall function (rainFunct) made by rainfall event pulses.
25  > rainn := convert(Column(drain, 2), list):
26  revent := [NULL]; raint := 0:
27  for i to nops(rainn) do
28  prec := convert(rainn[i], float):

```

```

1      if prec > 0 then
2          revent := [op(revent), [i, prec]]:
3          raint := raint+prec:
4      fi:
5      od:
6      rainFunct := t→sum(revent[jjk][2]*(-Heaviside(t-revent[jjk][1])+Heaviside(t-
7      revent[jjk][1]+1)), jjk = 1 .. nops(revent)):
8      ndata := nops(rainn);
9

```

10 4. We define the model equations.

```

11      > dB := gmax*(W-W0)*B/(W+kw)-m*B;
12      dW := P*(B+ki*i0)/(B+ki)-c*gmax*(W-W0)*B/(W+kw)-rw*W;
13      dsys := subs(W = W(t), B = B(t), [dB, dW]):
14      ecdif := [diff(B(t), t) = dsys[1], diff(W(t), t) = dsys[2]]:
15

```

16 5. We define a time-evolution function (evolution) that calculates and stores biomass values
17 for each day, integrating the model equations with the model parameter values.

```

18      > evolution := proc (param)
19          local stot, Biomassst, i:
20          stot := dsolve({op(subs(P = rainFunct(t), param, ecdif)), B(0) = 50, W(0) = .2}, numeric,
21          maxfun = 0):
22          Biomassst := NULL:
23          for i to ndata do
24              Biomassst := op([Biomassst]), subs(stot(i), B(t)):
25          od:
26          RETURN(Biomassst)

```

```

1      end proc:
2
3  6. We define the parameter values and call the time-evolution function.
4      > herbParam := W0 = 0.05, kw = 0.45, ki = 180, i0 = 0.2, c = 0.1, rw = 0.1, gmax = 0.32,
5      m = 0.05:
6      shrubParam := W0 = 0.05, kw = 0.45, ki = 180, i0 = 0.2, c = 0.1, rw = 0.1, gmax = 0.12, m
7      = 0.03:
8      herbBiomass := evolution({herbParam}):
9      shrubBiomass := evolution({shrubParam}):
10
11 7. We plot the time series of herbaceous and shrub biomass along with precipitation.
12      > topL := 700:
13      figherb := pointplot([seq([i, herbBiomass[i]], i = 1 .. nops([herbBiomass]))], connect =
14      true, color = green):
15      figshrub := pointplot([seq([i, shrubBiomass[i]], i = 1 .. nops([shrubBiomass]))], connect =
16      true, color = red):
17      figYears := [NULL]:
18      for iy to 16 do
19          figYears := [op(figYears), pointplot([[365*iy, 0], [365*iy, topL]], color = grey, connect =
20          true, linestyle = 3)]
21      od:
22      figPrecip := NULL:
23      for i to ndata do if drain[i][2] > 0 then
24          figPrecip := op([figPrecip]), pointplot([[i, topL], [i, topL-4*drain[i][2]]], connect = true,
25          color = navy, thickness = 3):
26      fi:
27      od:

```

```
1 figures:= display(figherb, figshrub, figYears, figPrecip):  
2 display(figures);  
3  
4 8. We export the output files.  
5 fout := cat(droot, "Biomass.txt");  
6 for i to ndata do  
7 FileTools[Text][WriteLine](fout, cat(dates[i][1], " ", convert(herbBiomass[i], string), " ",  
8 convert(shrubBiomass[i], string))):  
9 od:  
10 FileTools[Text][Close](fout);  
11 plotsetup(png, plotoutput = cat(droot, "Biomass.png")):  
12 display(figures);  
13 plotsetup(default):  
14
```

```

1  Code 2: NDVI Decomposition Procedure
2
3  Input files (location: C:\DataFolder\):
4    1. NDVI experimental data: case.txt
5    Data is stored in column 1.
6    2. Characteristic antecedent rainfall series for herbaceous and shrub vegetation ( $ARain_{hv}$  and
7        $ARain_s$ , respectively): totalAR.txt
8    Data is stored in columns 1 and 2 for herbaceous and shrub vegetation, respectively.
9    3. Time in days from the initial date: totalT.txt
10   Data is stored in column 1.
11
12  Output files (location: C:\DataFolder\):
13    1. Temporal series of herbaceous and shrub NDVI components: HScomponents.txt
14    Data is stored in columns 1 and 2 for herbaceous and shrub biomass, respectively.
15    2. Graph with the temporal series of herbaceous and shrub NDVI, along with the original total
16    NDVI signal: HScomponents.png (black, original signal; green, herbaceous component; red,
17    shrub component).
18
19  Procedure:
20  1. We load the Maple packages required for the subsequent calculations.
21    > with(ExcelTools): with(plots): with(plottools): with(LinearAlgebra): with(Statistics):
22
23  2. We define the NDVI bare soil component (0.12) and define a function, pair, to handle data
24  lists.
25    nsoil := 0.12;
26    pair := proc (x, y)
27      [x, y]
28    end proc

```

```

1
2 2. We load the data files and store data as lists. The following data lists are defined:
3 dataAR1 = antecedent rainfall series for herbaceous vegetation (57-day period,  $ARain_{hv}$ 
4 series).
5 dataAR2 = antecedent rainfall series for shrubs (145-day period,  $ARain_s$  series).
6 dataT = time (measured in days from the beginning of the series).
7 dataNDVI = original NDVI time series.
8 dataNDVI0 = NDVI data list without the soil base line.
9 > droot := "C:\\\\ DataFolder \\":
10 dNDVI := ImportMatrix(cat(droot, "case.txt"), source = delimited, delimiter = " ", 
11 datatype = anything);
12 totalAR := ImportMatrix(cat(droot, "TotalAR.txt"), source = delimited, delimiter = " ", 
13 datatype = anything);
14 totalT := ImportMatrix(cat(droot, "totalT.txt"), source = delimited, delimiter = " "):
15 Ndata := op(rtable_dims(dNDVI)[1])[2];
16 dataAR1 := [NULL]: dataAR2 := [NULL]: dataAR1N := [NULL]: dataAR2N := [NULL]: 
17 dataT := [NULL]: dataNDVI := [NULL]: dataNDVI0 := [NULL];
18 for i to Ndata do
19 dataAR1 := [op(dataAR1), evalf(totalAR[i][1])]: dataAR2 := [op(dataAR2),
20 evalf(totalAR[i][2])]: dataT := [op(dataT), evalf(totalT[i][1])]: dataNDVI := 
21 [op(dataNDVI), evalf(dNDVI[i][1])]: dataNDVI0 := [op(dataNDVI0), evalf(dNDVI[i][1]-
22 nsoil)]
23 od:
24
25 4. We define a first-order least-squares optimization function (linearfit) that fits the partial
26 contribution of the herbaceous and shrub components to the time series of NDVI (filtered for
27 the base-line bare soil contribution, dataNDVI0) as a function of the vegetation-type specific

```

1 *antecedent rainfall series that maximize the NDVI-precipitation relationships for herbaceous*
 2 *vegetation (dataAR1, ARain_{hv} series) and for shrubs (dataAR2, ARain_s series).*

3 >linearfit := proc (TAR1, TAR2, Tiemp, NDVIst)
 4 local AInput, DOutput, fitlinear, dparam, i, sumres;
 5 global Total;
 6 AInput := zip(pair, TAR1, TAR2); DOutput := NDVIst;
 7 fitlinear := LinearFit([ar1, ar2], AInput, DOutput, [ar1, ar2], output = solutionmodule);
 8 dparam := fitlinear:-Results("leastsquaresfunction"); sumres := fitlinear:-
 9 Results("residualsumofsquares");
 10 Total := [NULL]; for i to Ndata do Total := [op(Total), subs(ar1 = AInput[i][1], ar2 =
 11 AInput[i][2], dparam+nsoil)] od:
 12 RETURN(dparam, sumres);
 13 end proc;

14

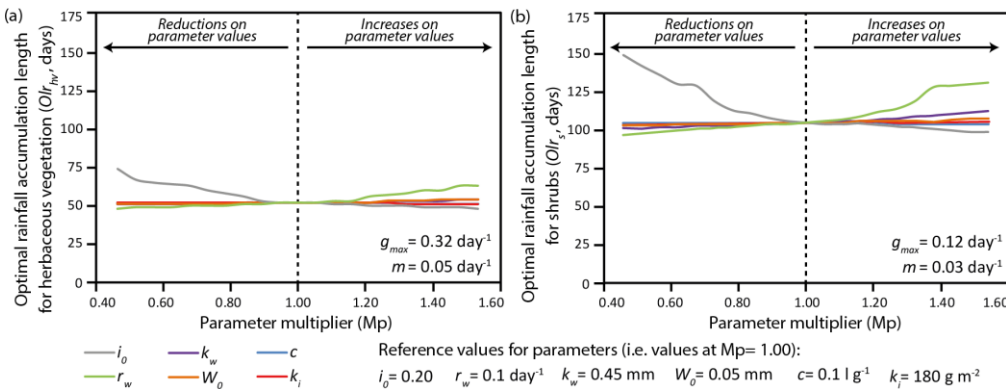
15 5. We define a function that reassigns the predicted weights of the fitted vegetation
 16 components (i.e. the percentage contribution of each vegetation type over the predicted totals
 17 for any t_i) to match the original shape of the NDVI time series, obtaining the final NDVI
 18 components for herbaceous vegetation and shrubs.

19 > linDecomp := proc (TAR1, TAR2, NDVIst, fit)
 20 local Ntotal, j, i, pre1, pre2, ratio;
 21 global Nherb, Nshrub;
 22 Nherb := [NULL]; Nshrub := [NULL]; Ntotal := [NULL];
 23 for i to Ndata do
 24 pre1 := subs(ar1 = TAR1[i], ar2 = 0, fit); pre2 := subs(ar1 = 0, ar2 = TAR2[i], fit);
 25 if 0 <= pre1 and 0 <= pre2 then ratio := NDVIst[i]/subs(ar1 = TAR1[i], ar2 = TAR2[i], fit);
 26 Ngrass := [op(Nherb), pre1*ratio]; Nshrub := [op(Nshrub), pre2*ratio] elif pre1 < 0 and 0
 27 <= pre2 then Nherb := [op(Nherb), 0]; Nshrub := [op(Nshrub), NDVIst[i]] elif pre2 < 0
 28 and 0 <= pre1 then Nherb := [op(Nherb), NDVIst[i]]; Nshrub := [op([Nshrub]), 0] else
 29 print(errors); ratio := 1; Nherb := [op(Nherb), 0]; Nshrub := [op(Nshrub), 0] fi;
 30 Ntotal := [op(Ntotal), Nherb[nops(Nherb)]+Nshrub[nops(Nshrub)]+nsoil] od;
 31 RETURN(Nherb, Nshrub, Ntotal);
 32 end proc;

```

1
2 6. We call the fitting and reassigning functions.
3 lfit1 := linearfit(dataAR1, dataAR2, dataT, dataNDVI0);
4 HerbShrubLineal := linDecomp(dataAR1, dataAR2, dataNDVI0, lfit1[1]);
5
6 7. We plot the time series of the NDVI signal (figOr), and the final NDVI components for
7 herbaceous vegetation (figHerb) and shrubs (figShrub).
8 figOr := PLOT(CURVES(convert(sort(zip(pair, dataT, dataNDVI)), list)));
9 figHerb := PLOT(CURVES(sort(sort(zip(pair, dataT, Nherb)))), COLOR(RGB, 0, 1, 0));
10 figShrub := PLOT(CURVES(sort(sort(zip(pair, dataT, Nshrub)))), COLOR(RGB, 1, 0, 0));
11 display(figOr, figHerb, figShrub);
12
13 8. We export the output files.
14 fout := cat(droot, "HScomponents.txt");
15 for i to Ndata do
16 FileTools[Text][WriteLine](fout, cat(convert(Nherb[i], string), " ", convert(Nshrub[i],
17 string)));
18 od;
19 FileTools[Text][Close](fout);
20 plotsetup(png, plotoutput = cat(droot, "HScomponents.png"));
21 display(figOr, figHerb, figShrub);
22 plotsetup(default);
23

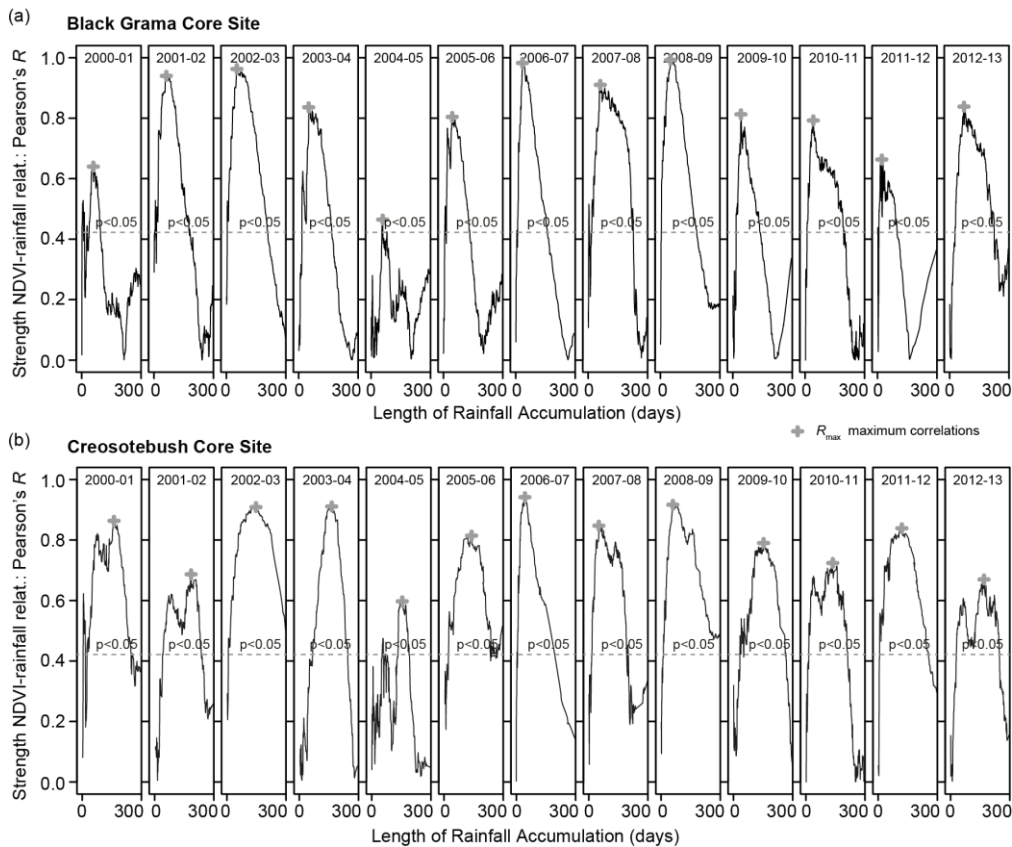
```



2 **Supplementary Fig. 1. Sensitivity of simulated Olr values for herbaceous vegetation (a,**
3 **Olr_{hv}) and shrubs (b, Olr_s) to variations in model parameters i_0 (bare soil infiltration rate), r_w**
4 **(soil moisture evaporation/deep drainage rate), k_w (vegetation growth half saturation**
5 **constant), W_0 (permanent wilting point), c (plant-water-consumption coefficient), and k_i**
6 **(water infiltration half saturation constant). Parameter values applied in this study are shown**
7 **in the figure (i.e. reference values). Parameter variations to the reference values are**
8 **represented by the parameter multiplier (Mp), with Mp values <1 (and >1) showing**
9 **reductions (and increases) on parameter values. Maximum growth (g_{max}) and mortality (m)**
10 **rates applied in the study for herbaceous vegetation and shrubs are detailed within the plots.**

11 **Notes:**

12 **Variations on W_0 , k_w , k_i , and c values have negligible effects on simulated Olr . Reductions on**
13 **bare soil infiltration (i_0) and increases on water loss by direct evaporation and/or deep**
14 **drainage (r_w) impact Olr_{hv} and Olr_s values, increasing time scale responses of vegetation to**
15 **antecedent precipitation, and ultimately amplifying the differences we obtained between**
16 **vegetation types.**



1 **Supplementary Fig. 2.** Per annual growing cycle (April-March) NDVI-antecedent rainfall
2 correlograms for the (a) Black Grama and (b) Creosotebush SEV LTER Core Sites.

Deleted: 1

3 **Notes:**
4 Correlations between NDVI and antecedent precipitation are maximized using a rainfall
5 accumulation length of about 57 days for all annual cycles of vegetation growth in the Black
6 Grama Core Site (Supplementary Fig. 2a).
7 For the Creosotebush Core Site two different foci that maximize the correlation between
8 NDVI and antecedent rainfall can be detected: (i) one using a low rainfall accumulation
9 length (approx. 57 days) and (ii) another using a long rainfall accumulation length (approx.
10 145 days). The 145 days antecedent rainfall series generally shows a stronger correlation with
11 the NDVI than the 57 days antecedent rainfall series (cycles 2000-01, 2001-02, 2002-03,
12 2003-04, 2004-05, 2009-10, 2010-11, 2011-12, 2012-13). However, for three consecutive
13 annual cycles with strong summer precipitation (2006-07, 2007-08, and 2008-09, summer
14 precipitation for the period is 40% above the long-term mean) correlation of NDVI to the 57

Deleted: 1

Formatted: Left, Space Before: 0 pt,
 Don't suppress line numbers

Deleted: the

1 days antecedent rainfall series is stronger than [n correlation](#) to the 145 days antecedent rainfall
2 series (Supplementary Fig. 2b).

Deleted: 1

Deleted: 1

Deleted: 1